NGU Report 99.129

Rutile deposits in Norway. Vol. 2: Figures

REPORT

Geological Survey of Norway
N-7441 Trondheim, Norway
Tel.: 47 73 90 40 11
Telefax 47 73 92 16 20

NGU
Norges geologiske undersøkelse
Geological Survey of Norway

Report no.: 99.129 | ISSN 0800-3416 | Grading: Åpen

Title:
Rutile deposits in Norway. Vol. 2: Figures.

Authors:
Korneliussen, A., Furuhaug., L., Gautneb, H. & Ihlen, P.

Client:
Rio Tinto Iron & Titanium

County:
Norway

Commune:

Map-sheet name (M=1:250.000)

Map-sheet no. and -name (M=1:50.000)

Deposit name and grid-reference:

Number of pages: 40 Price (NOK): Kr. 330,-
Map enclosures:

Fieldwork carried out:	Date of report:	Project no.:	Person responsible:
1989-94, 1999	14 Dec. 1999	284700	

Summary:

See the text in Report 99.129, Vol. 1.

Keywords: Mineral resources	Rutile	eclogite
Metamorphism	Metasomatism	albitite
fagrapport		

CONTENTS

Figures

Fe-Ti deposits in Norway

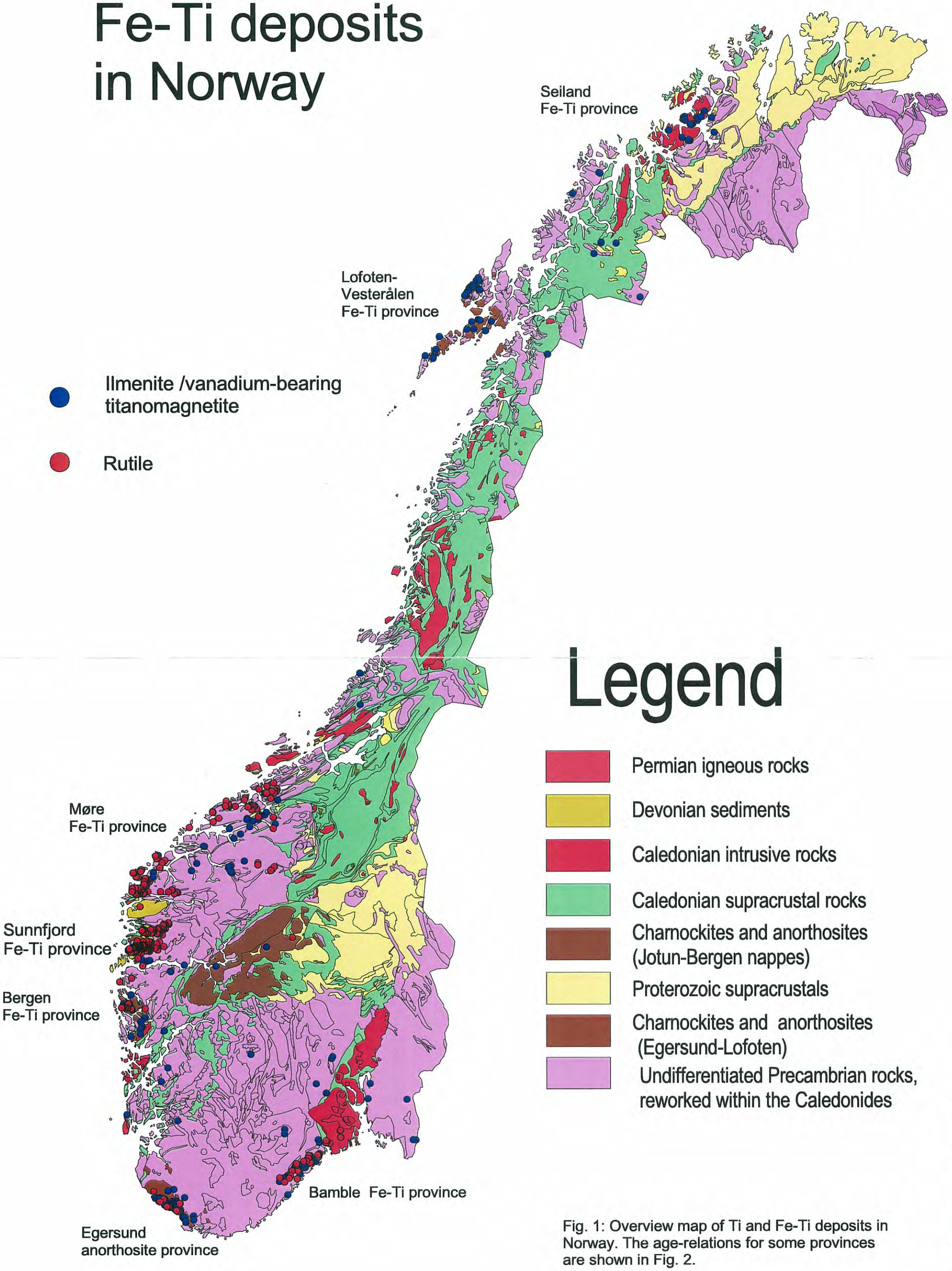

Fig. 1: Overview map of Ti and Fe-Ti deposits in Norway. The age-relations for some provinces are shown in Fig. 2.

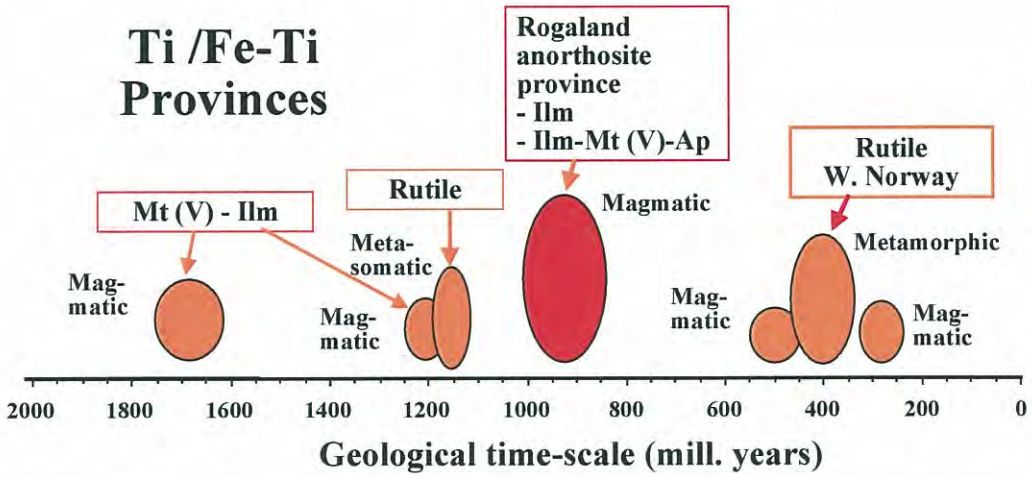

Fig. 2: Ti and Fe-Ti provinces in Norway vs. geological time. Rutile deposits are found in two provinces: the Bamble province (Chapt. 3.11) which formed around 1150 Ma, and rutile-bearing eclogites in Western Norway (Chapt. 3.1 – 3.10) formed at 400 Ma. See Nilsson et al. (1999) and Korneliussen et al. (in prep.) for additional information of Ti/Fe-Ti provinces in Norway.

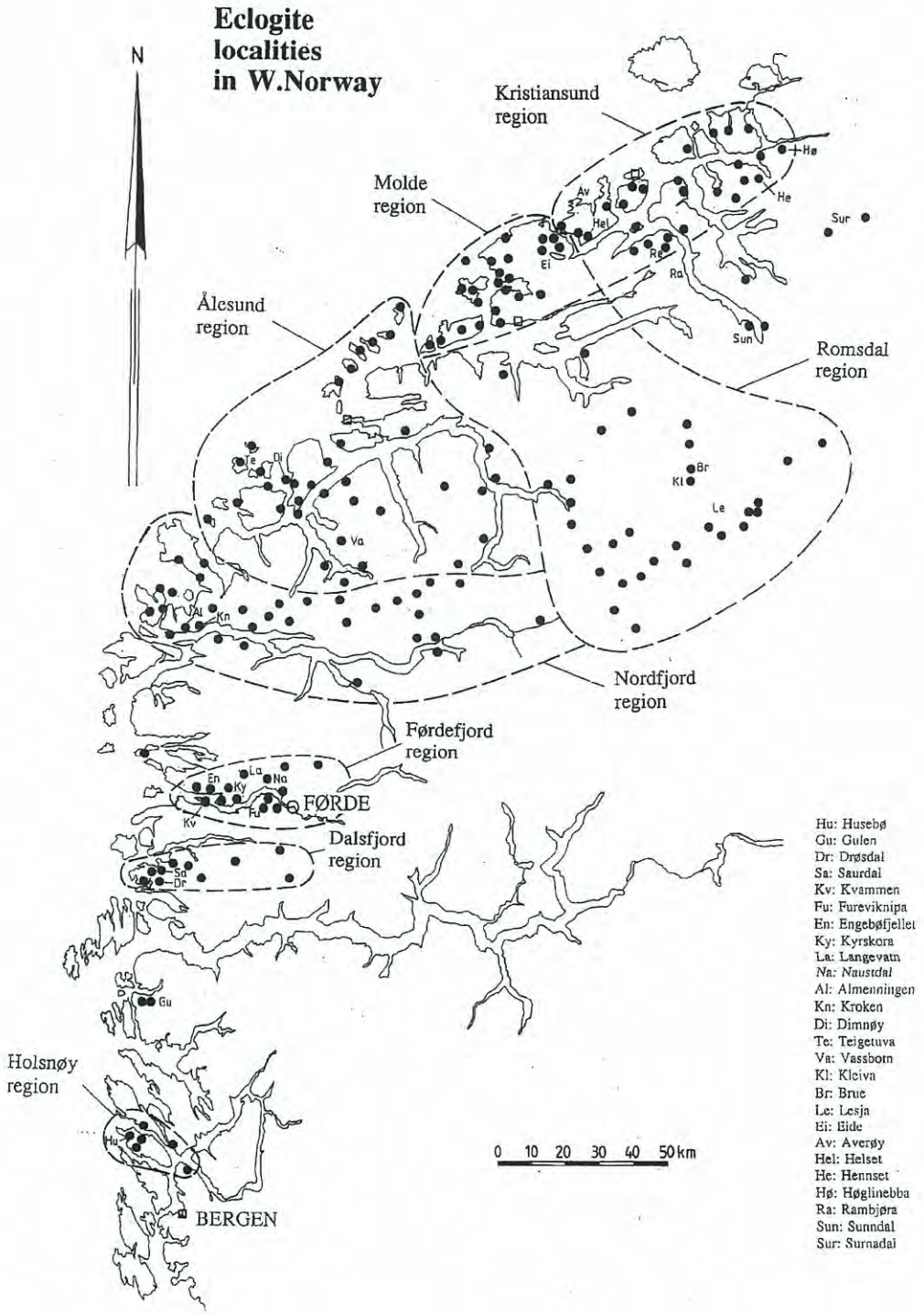

Fig. 3: General overview of the eclogite occurrences in Western Norway with subdivision in eclogite provinces (from Korneliussen 1994). The eclogite location map is modified from Griffin & Mørk (1981) and Erambert (1991).

Rutile deposits in Norway

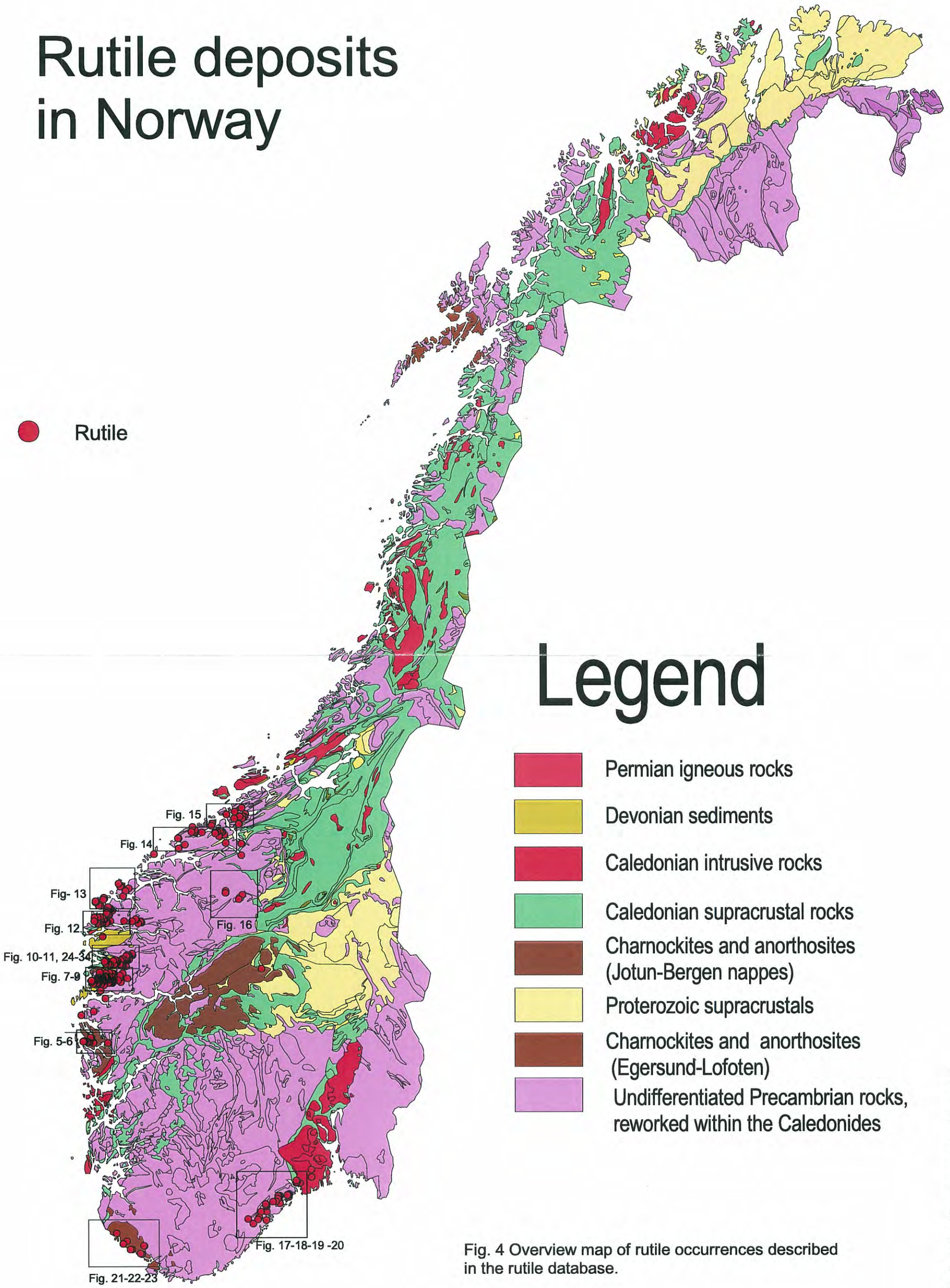

Fig. 4 Overview map of rutile occurrences described in the rutile database.

Fig. 6 →

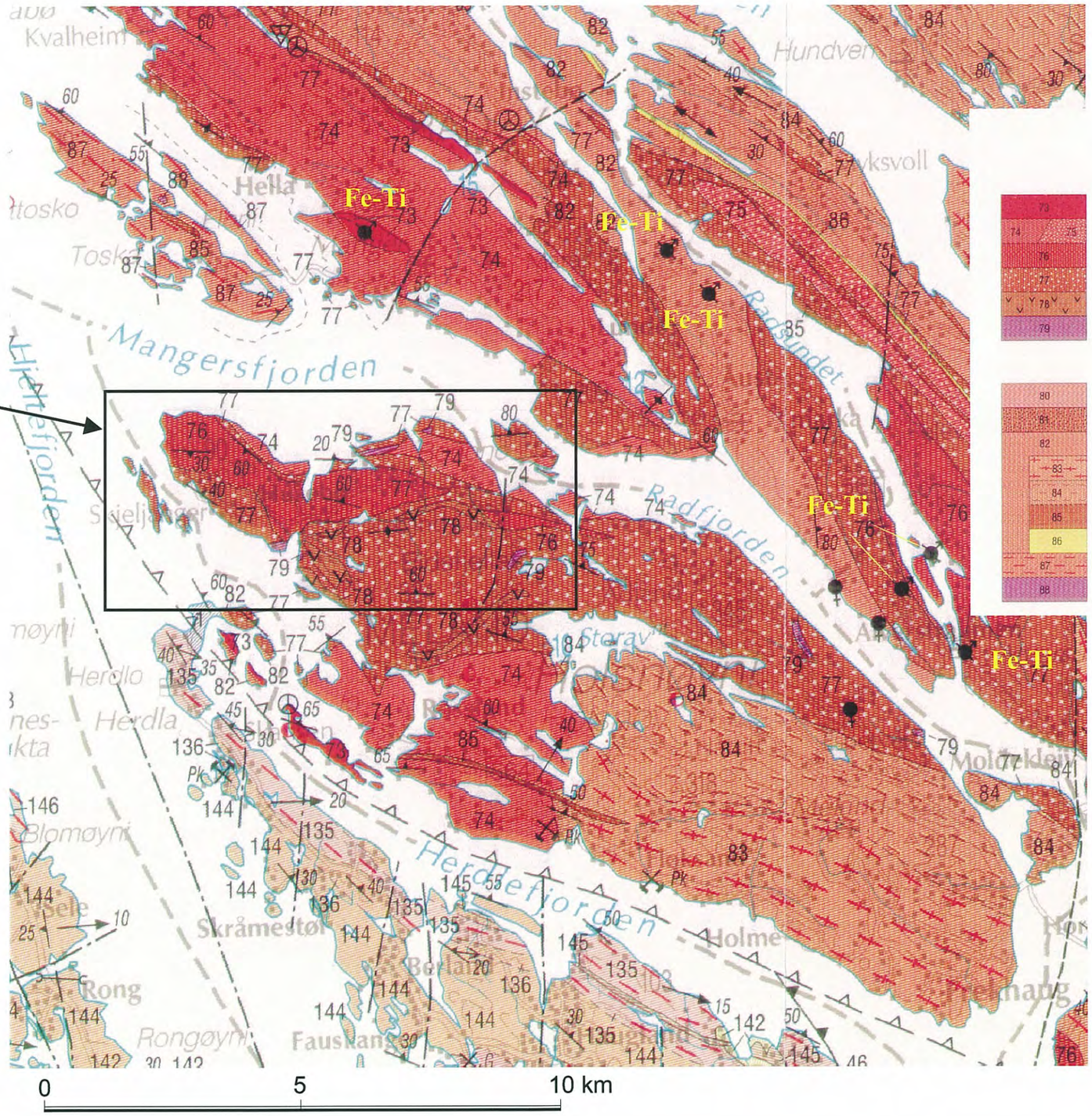

Lindåsdekket; omdannede bergarter fra proterozoisk tid, stedvis også omdannet under den kaledonske fjellkjededannelsen

Holsnøysuiten; charnockitt-/granulittbergarter, stedvis omdannet under den kaledonske fjellkjededannelsen

- Hyperstensyenitt til hypersten-kvartssyenitt, stedvis kaledonsk forgneiset
- Hyperstenmonzonitt til monzodioritt (mangeritt) / Mangeritt, kaledonsk forgneiset
- Monzonoritt (jotunitt), stedvis kaledonsk forgneiset
- Anortositt, stedvis også gabbro
- Metagabbro, stedvis også anortositt
- Ultramafiske bergarter (pyroksenitt, lherzolitt)

Bergarter for det meste tilhørende Holsnøysuiten, også eldre og yngre bergarter, omdannet under den kaledonske fjellkjededannelsen

- Granitt, rød, stedvis med koronateksturer av granataggregater
- Amfibolitt, finkornet
- Gneis og amfibolitt, stedvis båndet, stedvis migmatittisk
- Granittisk gneis, stedvis med mesoperthitt, også amfibolrik gneis og amfibolitt
- Amfibolrik gneis til amfibolitt, stedvis granittisk gneis
- Amfibolitt, stedvis forgneiset, grovkornet
- Kvartsittisk bergart av usikker opprinnelse, stedvis antatt kvartsitt
- Kvarts- og feltspatrik gneis, båndet
- Ultramafiske bergarter, vesentlig serpentinitt

Fig. 5: Overview geological map of the north-western part of the Bergen region, after Ragnhildstveit & Helliksen (1997). The black dots labelled "Fe-Ti" are deposits of ilmenite and titanomagnetite.

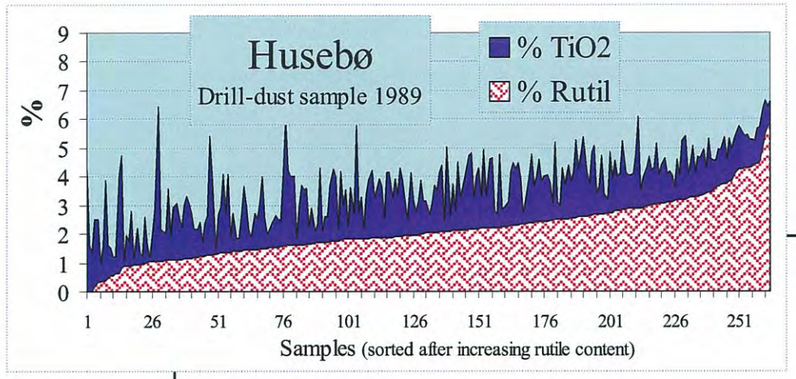

③

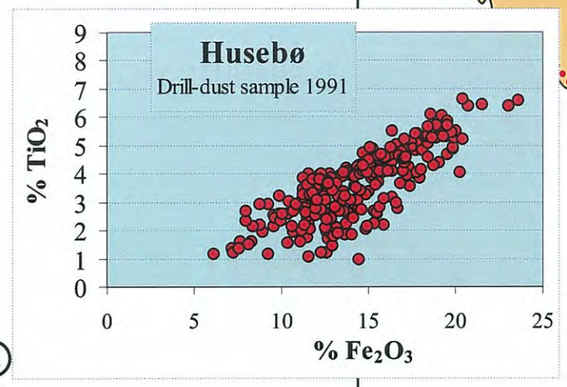

②

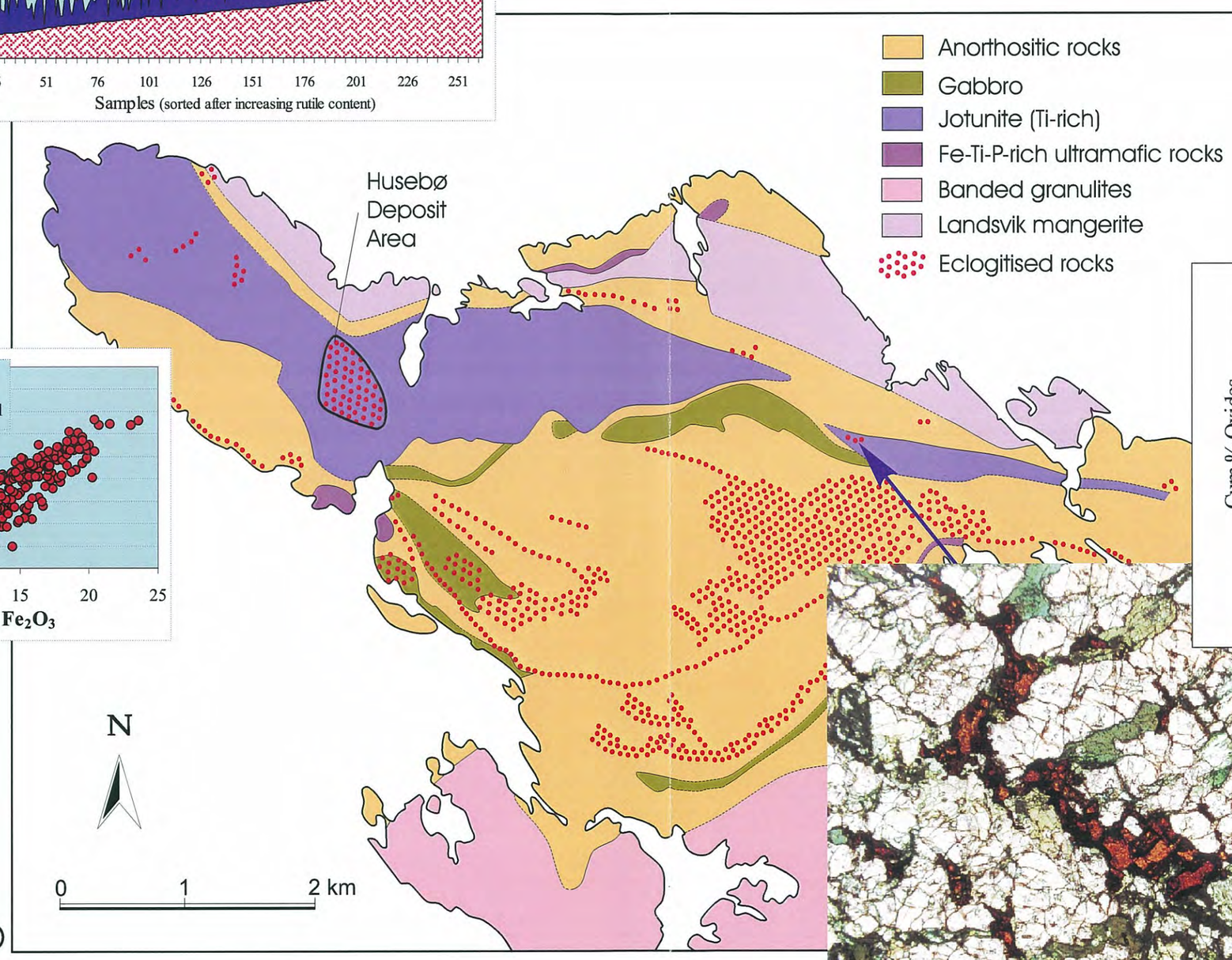

①

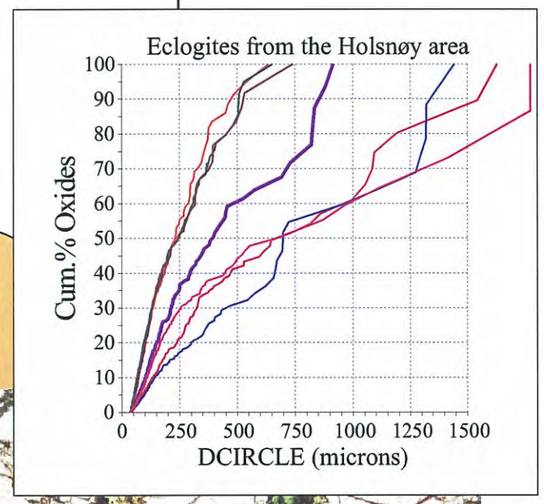

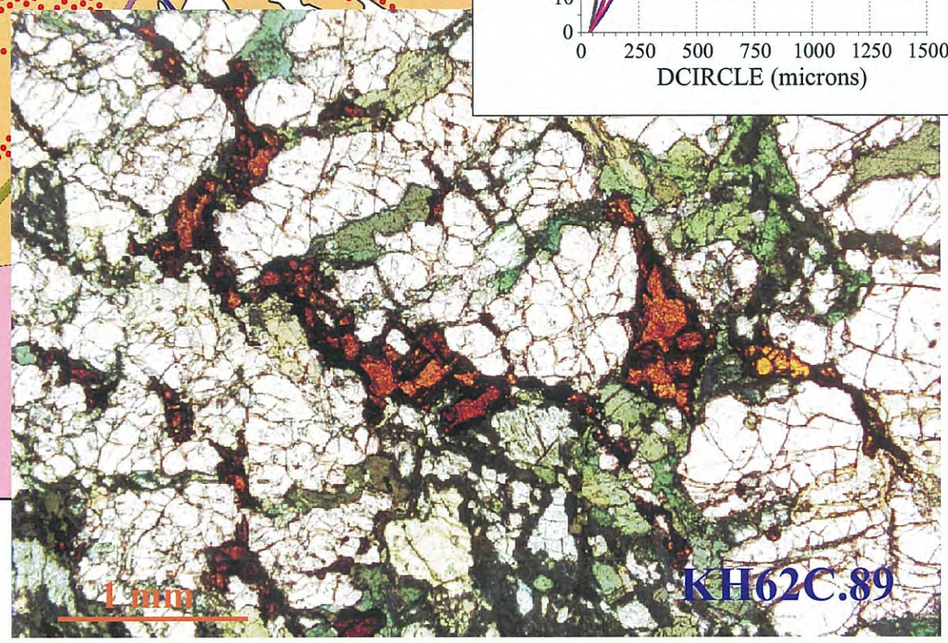

④

Fig. 6: Geological map of Holsnøy (1), based on a map by Håkon Austrheim in Korneliussen et. al 1990. The scattergram Fe_2O_3 – TiO_2 plot (2) is of drill-dust samples from the Husebø deposit (Korneliussen et. al 1990). The line/area plot (3) shows the rutile- and TiO_2 content in the same drill-dust samples which are sorted after increasing rutile content. The microphotograph (4) is an example of a typical, coarse-grained eclogite from Holsnøy, while (5) shown the cumulative grain-size distribution curves for a variety of eclogite samples (thin-section) from Holsnøy.

Eclogite localities in the western part (Langsjøen, Gjølanger and Flekke areas) of the Dalsfjord region.

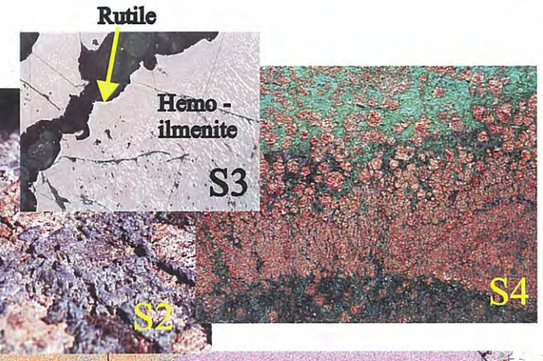

Photos to the left. S1: Overview photo of the Saurdal eclogite seen from the northeast.S2: Partly eclogitized and ther retrograde amphibolitic rock with relics of magmatic Fe-Ti oxides (black). S3: Microphoto of the oxide association of Fig. S2 showing rutile rimming hemo-ilmenite. In this case the eclogitization process that leads to decomposition of he mo-ilmenite and the formation of rutil, was incomplete. S4 Coarse-grained eclogite from a small dimention-stone quar ry (closed) on the southern slopes of the eclogite body (not seen in Fig. S1).Minerals seen are garnet (brownish red), o phacite (bright green),amphibole (dark green), rutile (black

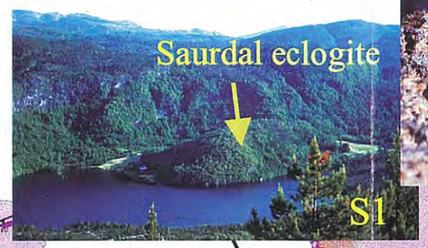

Right: Boudinaged eclogite dyke in granitoid gneiss. Scale by the coin.

Below at right: Extremely coarsegrained, partly eclogitized metagabbro with well-preserved relics of orthopuroxene (dark gray to black) and plagioclase (white).The red mineral is garnet. Scale by the coin.

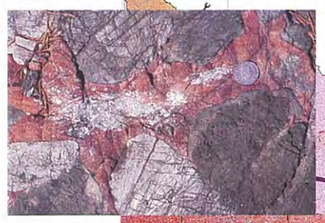

Below: Finely banded mafic to intermediate rock of unknown origin. Similar rocks has been called "metagabbro", "sheared metagabbro", "basite", "metabasite" at various occations.

Legend

Younger granitic rocks, Sveconorwegian

- Granitic gneiss, coarse-grained, red
- Granitic gneiss, mainly red, also more heterogenous pale red to grey with or without heterogenous gneiss-amphibolite remnants, mostly banded, locally migmatitic

Gjølanger unit, mid Proterozoic (?)

- Granodioritic to tonalitic and granitic gneiss with granitic dykes
- Tonalitic to dioritic gneiss, partly eclogitized ("green gneiss")
- Mainly tonalitic to dioritic gneiss

Flekke unit, mid Proterozoic (?)

- Eclogite
- Eclogite, intermediate to basic
- Amphibolite, mainly banded, partly altered gabbro, partly uncertain origin
- Amphibolite, metagabbro, locally altered leucogabbro to anorthosite
- Metagabbro, partly eclogitized
- Ultramafic rock

Proterozoic rocks with strong late Caledonian deformation

- Tonalitic to dioritic gneiss, granitic gneiss and amphibolite in varying amounts, heterogeneously mixed and/or banded
- Amphibolite and grey gneiss, banded, retrogressed
- Marble (uncertain age)

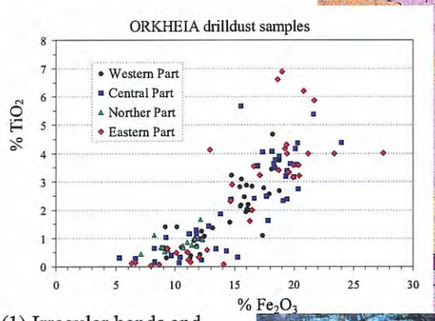

(1) Irregular bands and layers of dark, garnet -rich eclogite (dark brownish red) within an omphacite-rich eclogite (greenish), Orkheia.

(2) Dyke-like, dark, garnet- and Fe-Tirich eclogite surrounded by a finely banded eclogite with relatively low Fe-Ti content.

(3) Microphoto of elongated rutile aggregate, sample K153C.93, Orkheia.

(4) Microphoto of rutile in eclogite, sample K153C.93, Orkheia

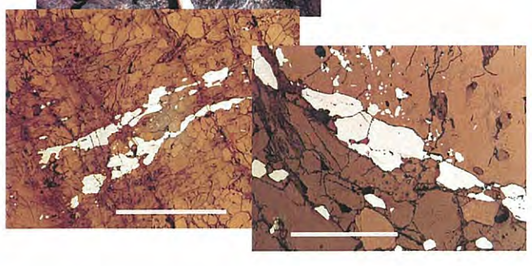

Fig. 7: Eclogites in the Western Dalsfjord region.

Western Dalsfjord region

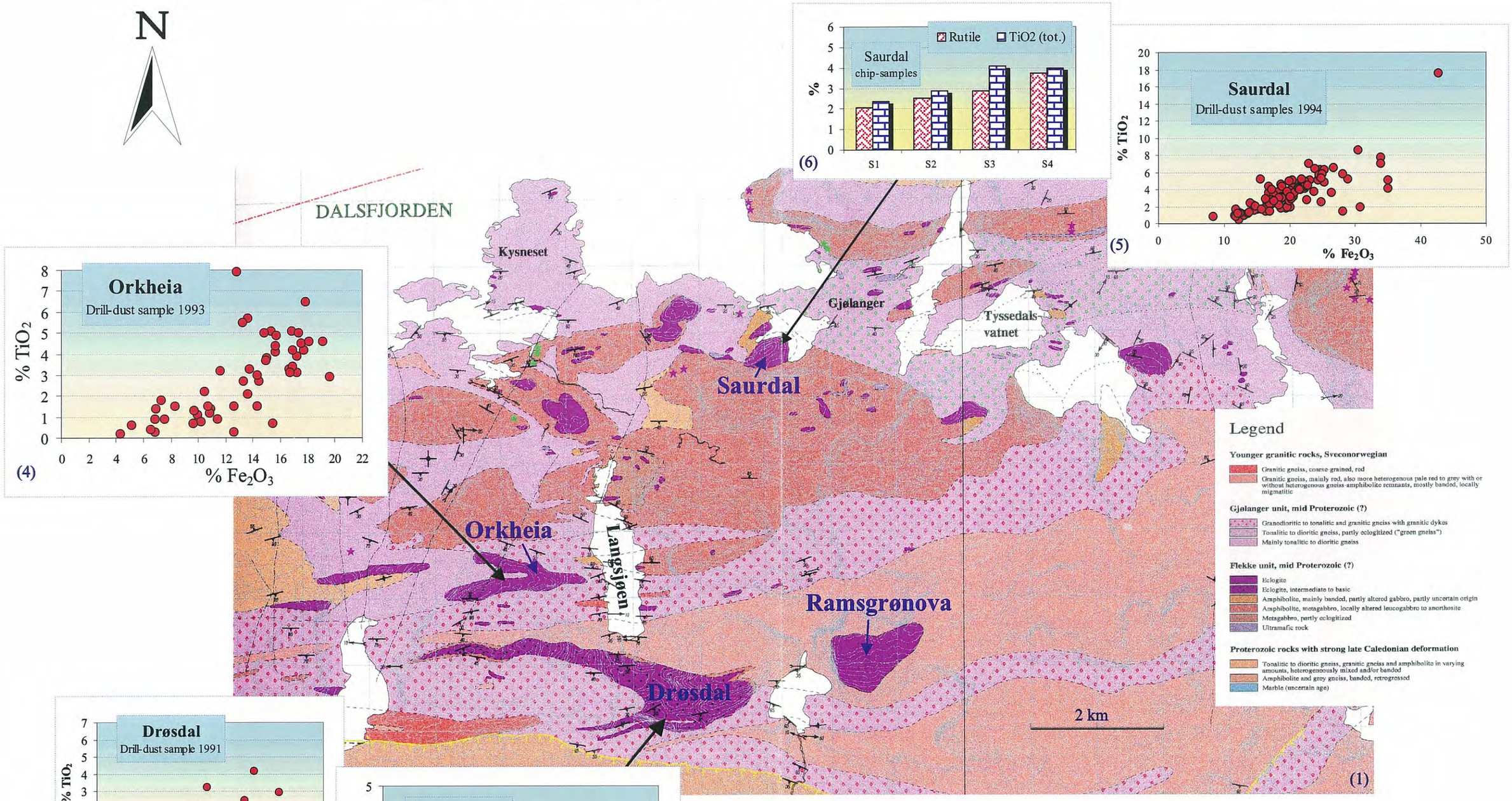

Fig. 8: Miscellaneous graphs, W. Dalsfjord region. The geological map (1) is from Ragnhildstveit (1998). The Fe_2O_3 – TiO_2 scattergram plot (2) and the line/area-plot are of drill-dust samples from the Drøsdal eclogite taken by NGU in 1991. The Fe_2O_3 – TiO_2 scattergram plot (4) is of drill-dust samples from Orkheia taken by the DuPont/NGU project in 1993. Results from follow-up investigations at Orkheia in 1995 as well as investigations of the Ramsgrønova eclogite the same year, is confidetial according to the DuPont – NGU agreement out 2000. The Fe_2O_3 scattergram plot (5) is of drill-dust samples taken over the Saurdal eclogite by DuPont/NGU in 1994, while the chip-sample shown in (6) were taken in 1993 in a dimension-stone quarry. The graphs are based on analyses given in Appendix 2.

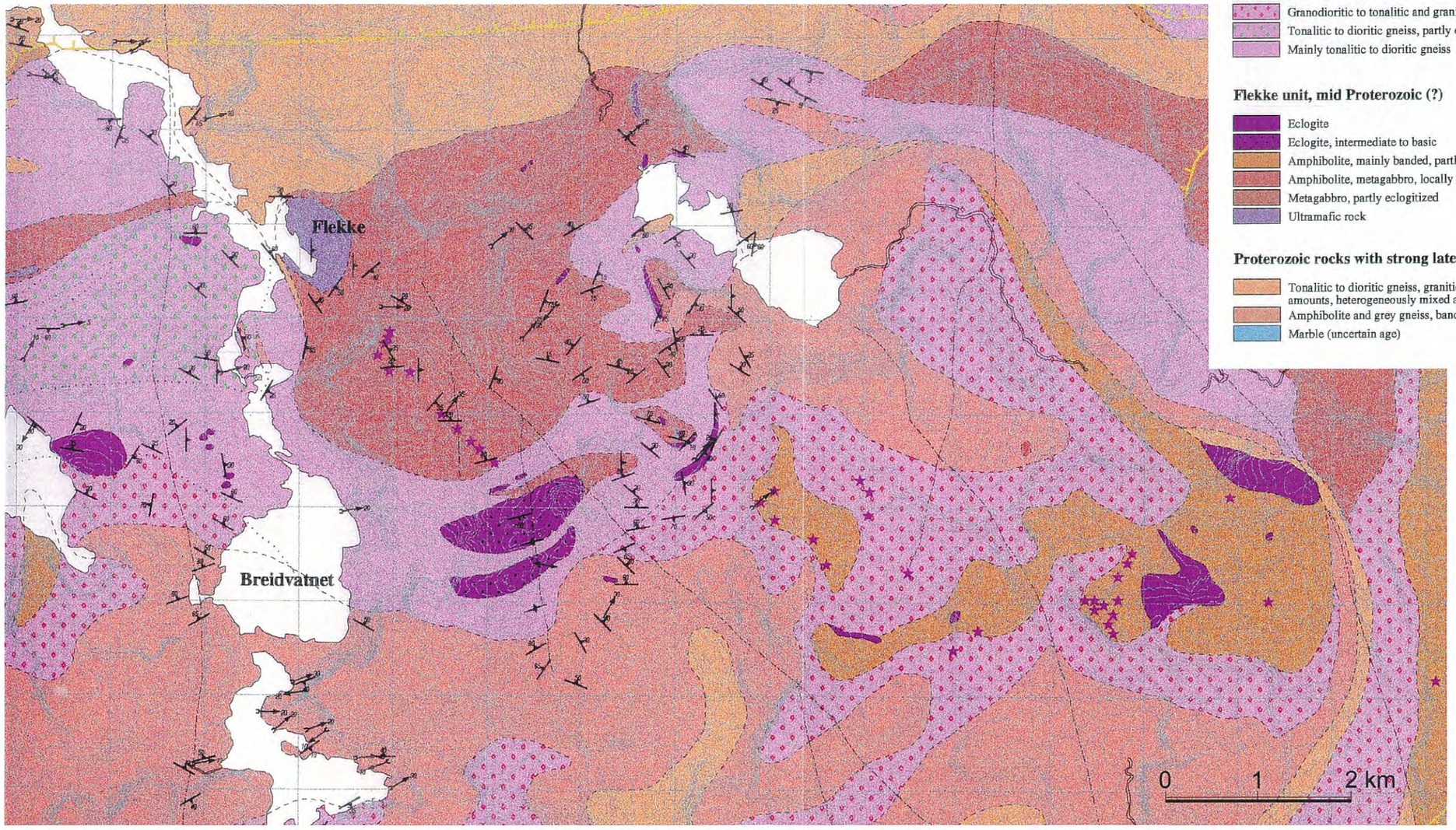

Legend

Younger granitic rocks, Sveconorwegian

- Granitic gneiss, coarse-grained, red
- Granitic gneiss, mainly red, also more heterogenous pale red to grey with or without heterogenous gneiss-amphibolite remnants, mostly banded, locally migmatitic

Gjølanger unit, mid Proterozoic (?)

- Granodioritic to tonalitic and granitic gneiss with granitic dykes
- Tonalitic to dioritic gneiss, partly eclogitized ("green gneiss")
- Mainly tonalitic to dioritic gneiss

Flekke unit, mid Proterozoic (?)

- Eclogite
- Eclogite, intermediate to basic
- Amphibolite, mainly banded, partly altered gabbro, partly uncertain origin
- Amphibolite, metagabbro, locally altered leucogabbro to anorthosite
- Metagabbro, partly eclogitized
- Ultramafic rock

Proterozoic rocks with strong late Caledonian deformation

- Tonalitic to dioritic gneiss, granitic gneiss and amphibolite in varying amounts, heterogeneously mixed and/or banded
- Amphibolite and grey gneiss, banded, retrogressed
- Marble (uncertain age)

Fig. 9: Eclogites in the Eastern Dalsfjord region, after Ragnhildstveit (1998).

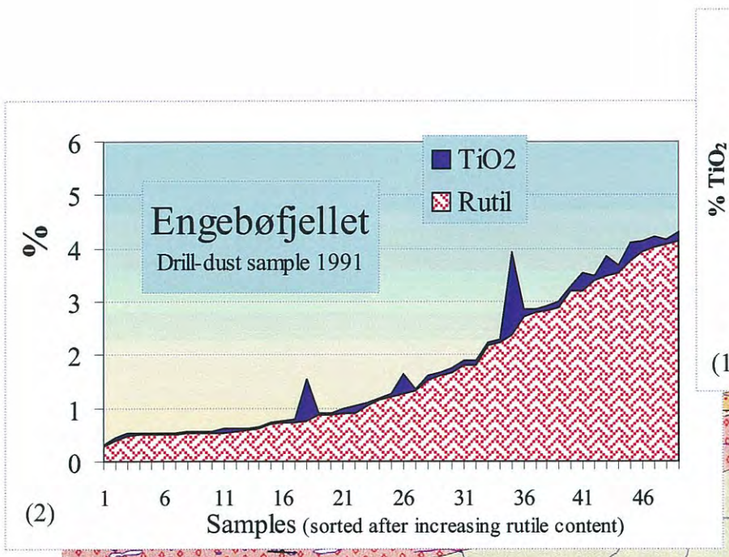

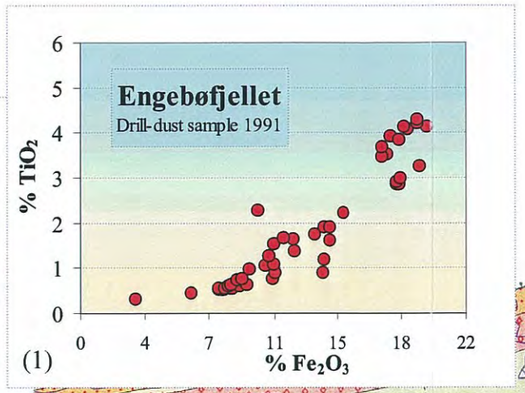

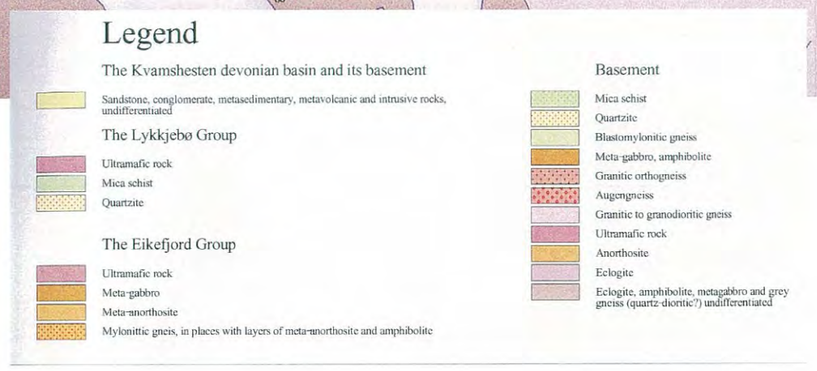

Fig. 10: Geologic map, Western Førdefjord region, from Lutro (1997). The scattergram Fe_2O_3 – TiO_2 plot (1) is from an East-West sample profile across Engebøfjell (Korneliussen and Furuhaug 1991). The line/area plot (2) is showing the rutile- and TiO_2 content in the same samples, sorted after increasing TiO_2 content. The graphs are based on analyses given in Appendix 2.

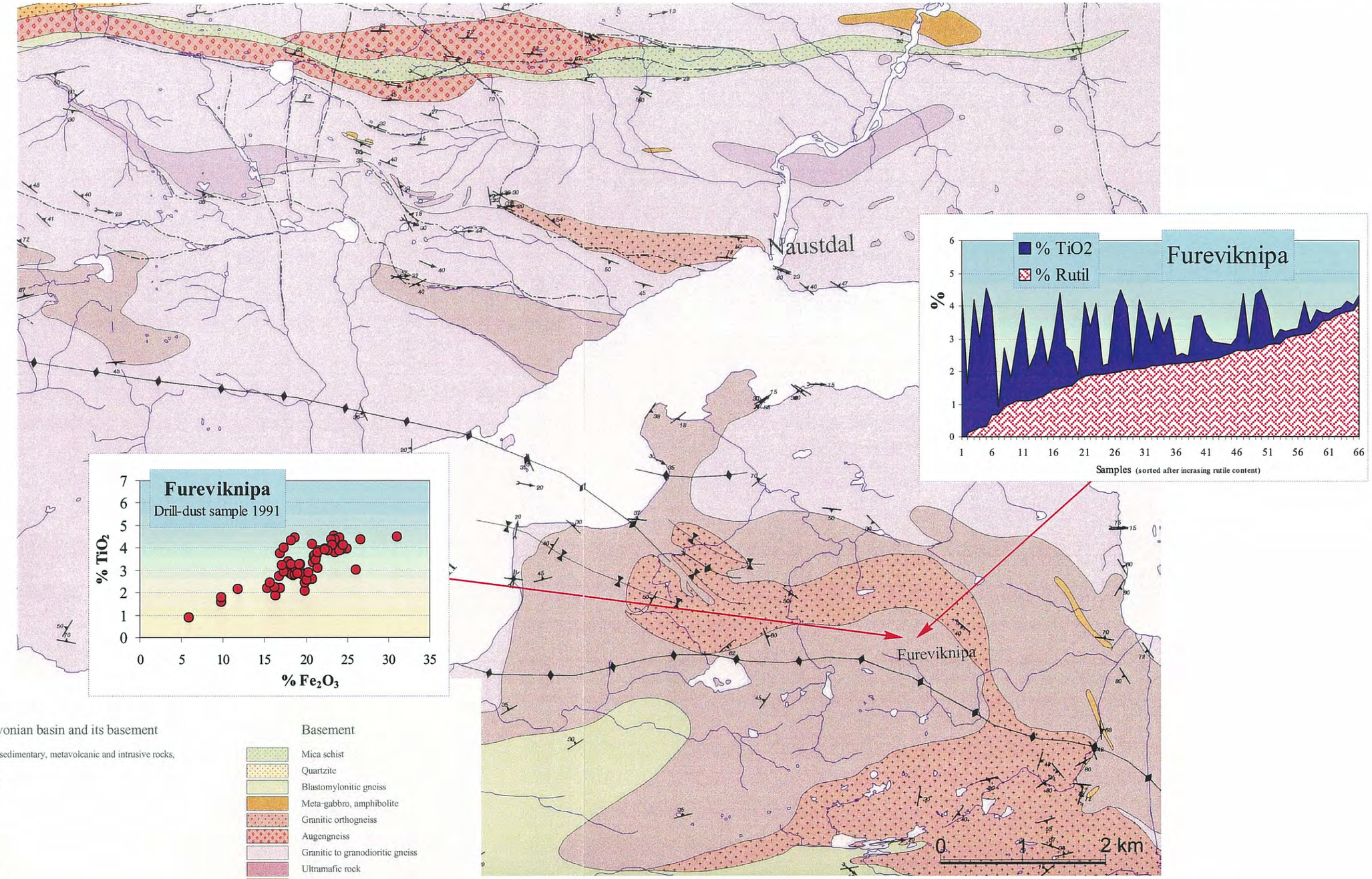

Fig. 11: Geological overview, Central Førdefjord region, from Lutro (1997). The graphs are based on analyses given in Appendix 2.

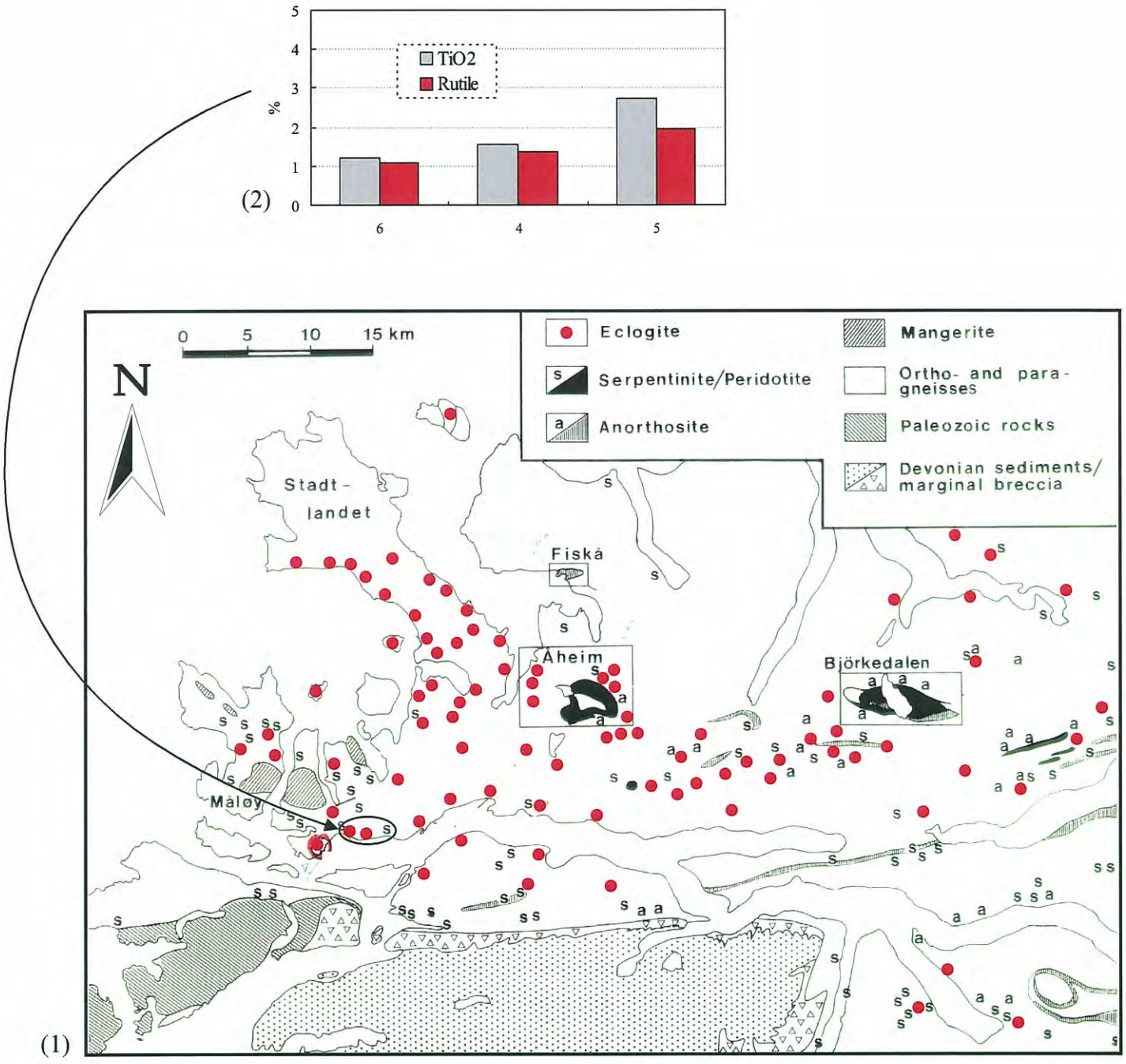

Fig. 12: Eclogites in the Nordfjord region. The map (1) is after Griffin & Mork (1981). The bar-graph (2) is showing the TiO_2- and rutile content in eclogite samples from an area on the northern side of Nordfjord.

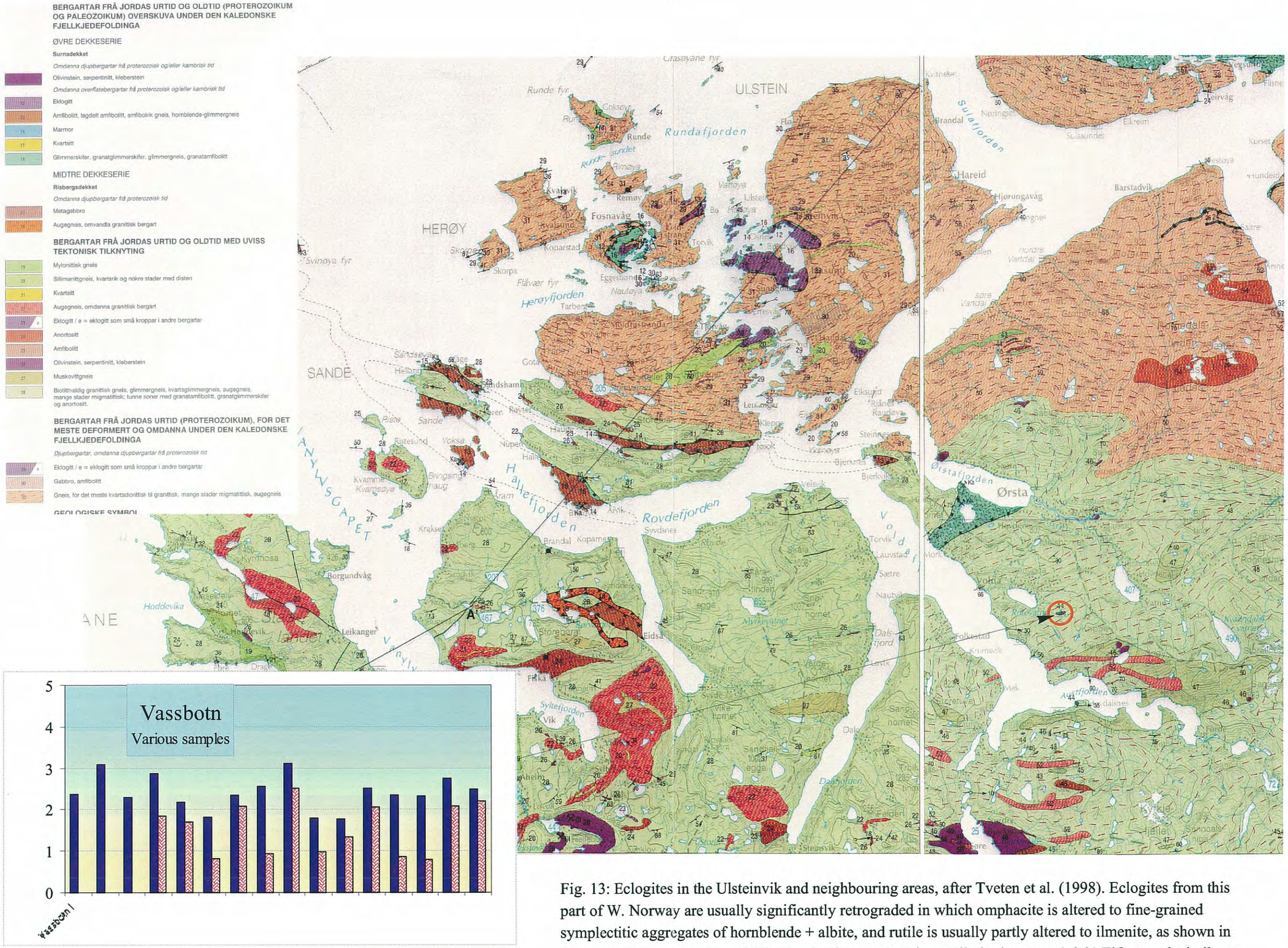

Fig. 13: Eclogites in the Ulsteinvik and neighbouring areas, after Tveten et al. (1998). Eclogites from this part of W. Norway are usually significantly retrograded in which omphacite is altered to fine-grained symplectitic aggregates of hornblende + albite, and rutile is usually partly altered to ilmenite, as shown in the microphotographs (3) and (4). The titanium content is usually in the range 1-3 % TiO_2, much similar to the eclogite analyses of the Vassbotn eclogite which are shown in the bar-graph (2). The analyses are given in Appendix 2.

(4)

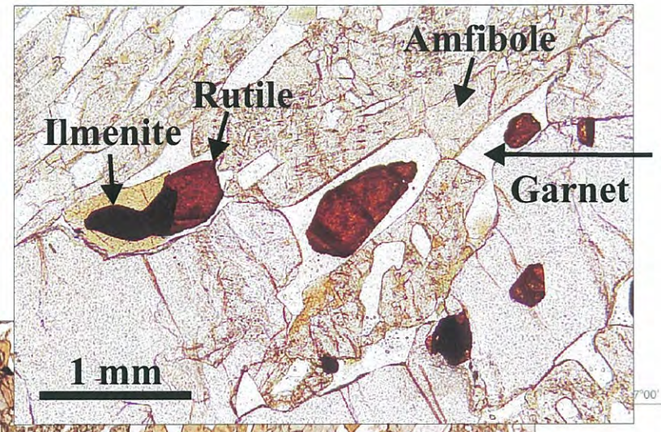

(2)

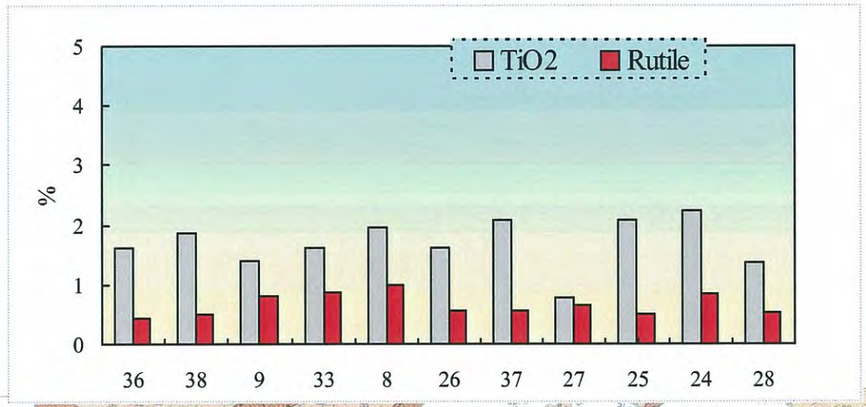

(3)

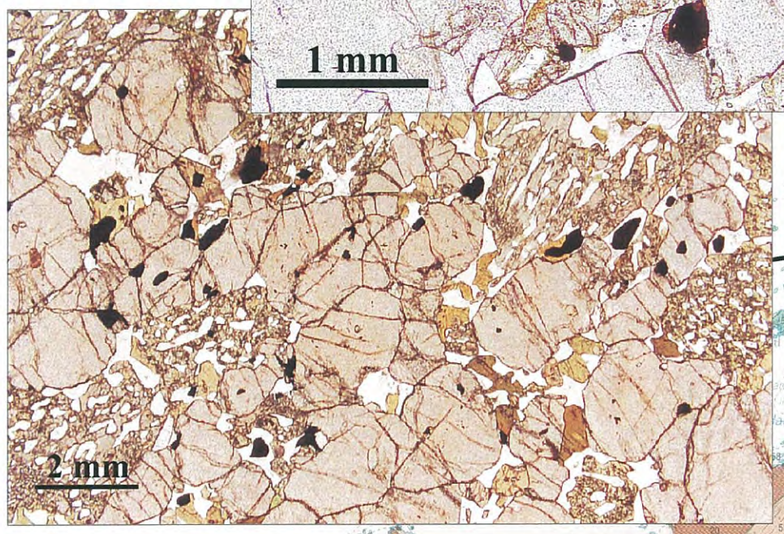

(1)

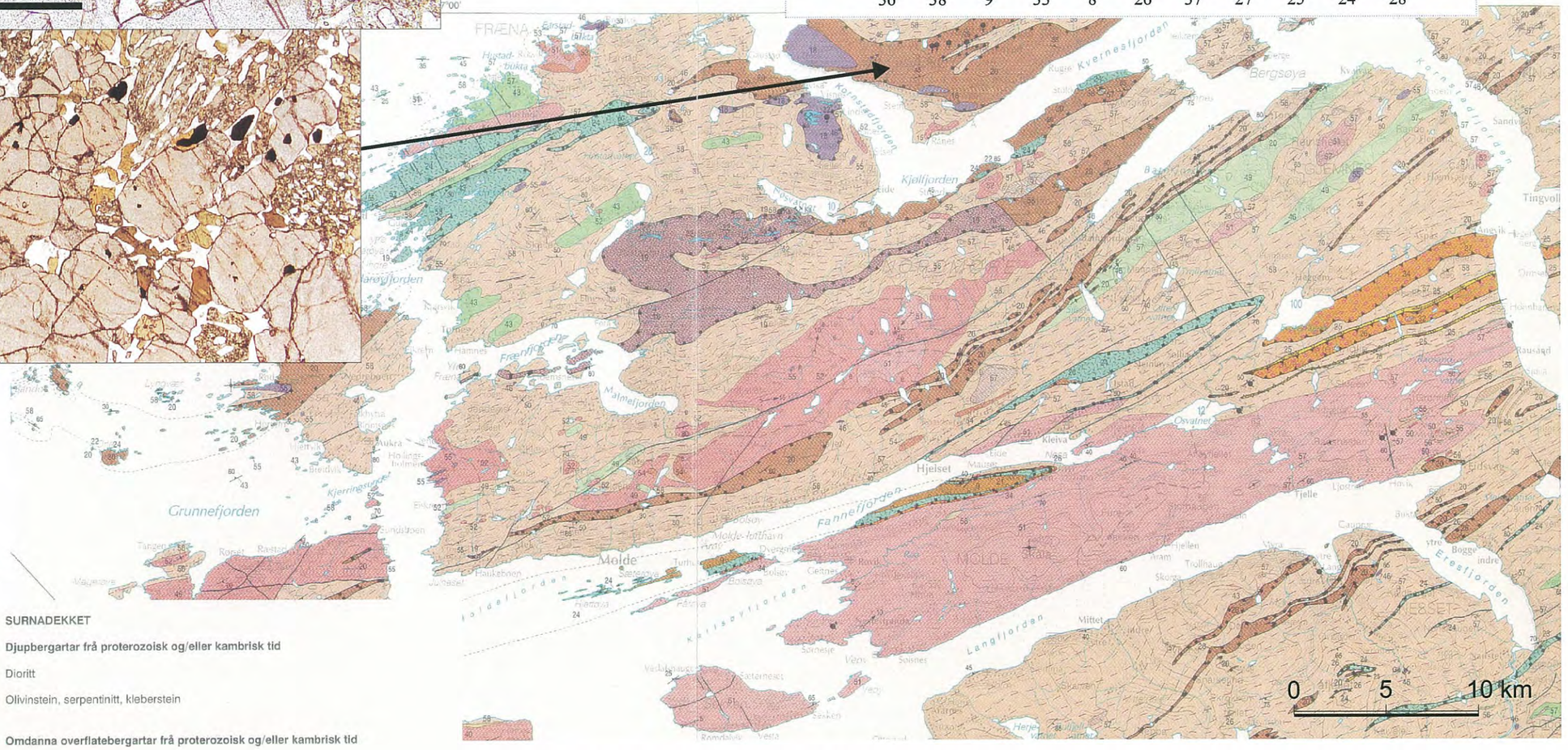

SURNADEKKET

Djupbergartar frå proterozoisk og/eller kambrisk tid

Dioritt

Olivinstein, serpentinitt, kleberstein

Omdanna overflatebergartar frå proterozoisk og/eller kambrisk tid

Eklogitt

Amfibolitt; omdanna eklogitt

Amfibolitt, lagdelt amfibolitt, amfibolrik gneis

Hornblende-glimmergneis

Marmor

Kvartsitt, nokre stader lagdelt

Glimmerskifer, granat-glimmerskifer, glimmergneis, granatamfibolitt; inneheld nokre stader linser og gangar av trondhjemitt og er nokre stader migmatittisk

Fig. 14: Eclogites in the Molde region. Numerous eclogites are found in the western and northern parts of the Molde region. Most of these are small occurences not marked in this map. In general the TiO_2-ratio is low, as shown in the bar-graph (2). The microphotographs in figures (3) and (4) are relatively representative examples of eclogites from the northern parts of the region. These eclogites are generally garnet-rich, other major silicates are omphacitic clinopyroxene, amphibole (formed by retrograde alteration of omphacite) and quartz. The rutile is commonly intergrown with ilmenite as shown in figure (4). The geological map (1) is from Tveten et al. (1998).

(3)

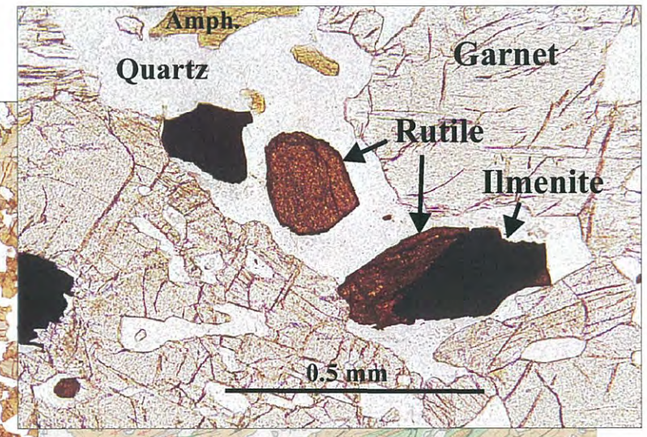

(2)

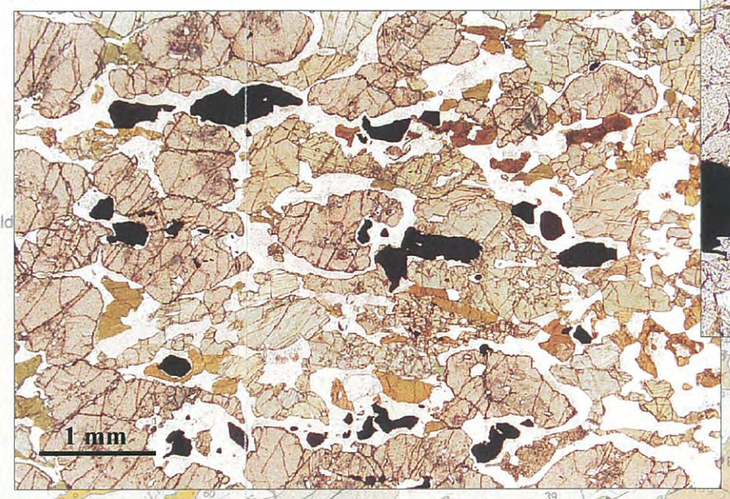

(1)

(4)

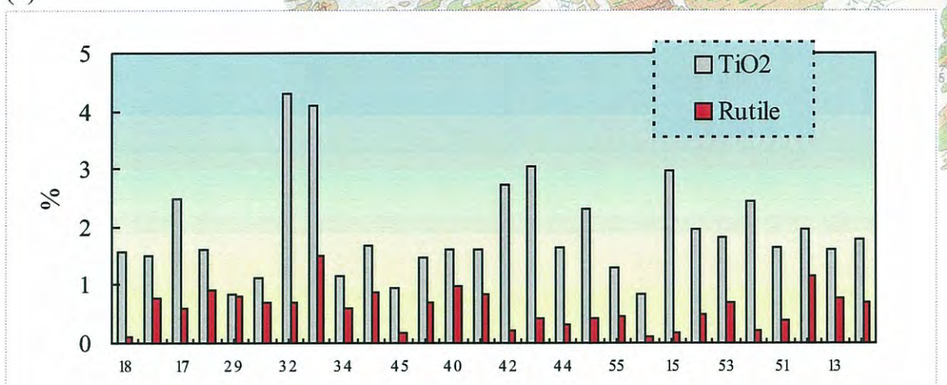

Fig. 15: Eclogites in the Kristiansund region, after Askvik og Rokoengen (1985). This region contains numerous eclogite, but most of these are small and not marked in this map. Retrograde alteration of eclogite to amphibolite is significant particularly in the north-eastern area. In the southern and south-eastern part of the map, gabbroic intrusions commonly show partly alteration to eclogite, particularly on the margin of the bodies and along shear-zones. The microphotographs (2) and (3) are representative for eclogites from the Kristiansund area and north-eastwards. Eclogites from this region have an overall low TiO_2-content as well as a low rutile/TiO_2-ratio, as shown in the bar-graph (4). The analyses used for this graph are given in Appendix 2.

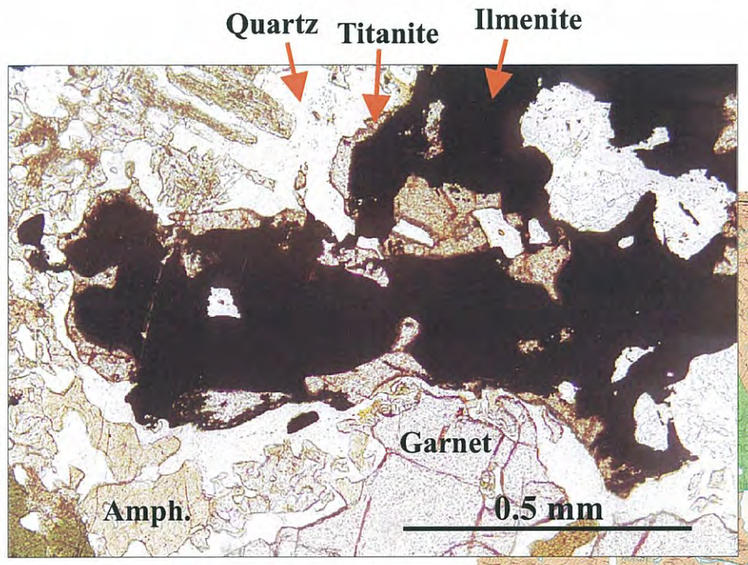

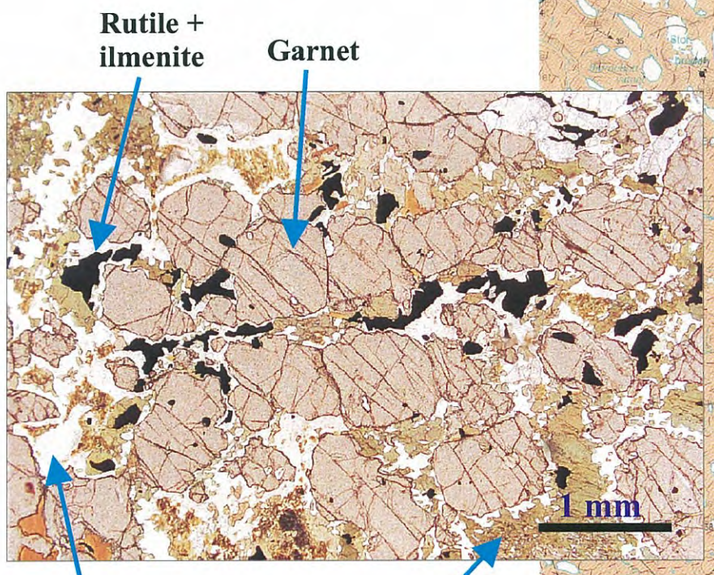

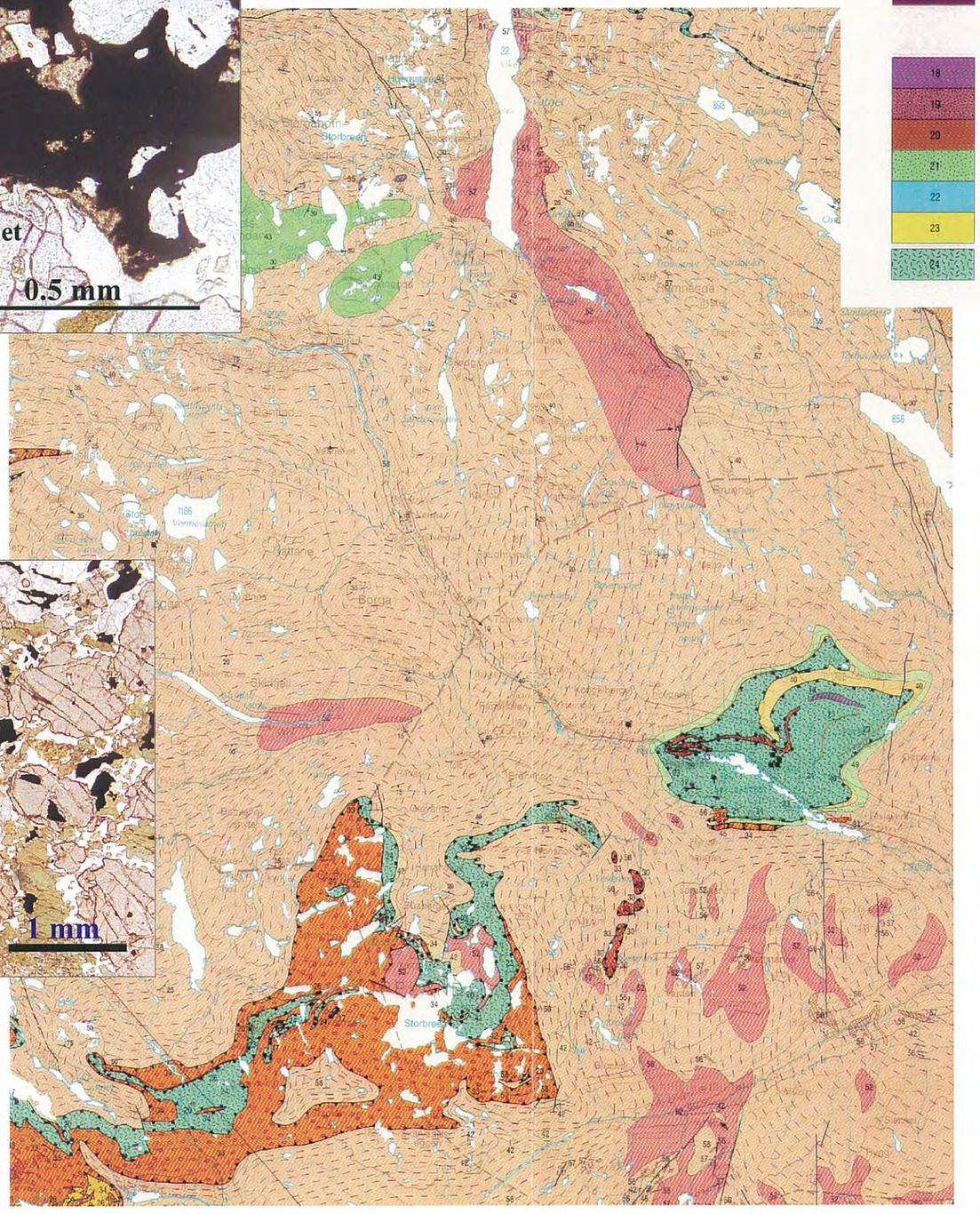

SURNADEKKET

Djupbergartar frå proterozoisk og/eller kambrisk tid

16 Dioritt

17 Olivinstein, serpentinitt, kleberstein

Omdanna overflatebergartar frå proterozoisk og/eller kambrisk tid

18 Eklogitt

19 Amfibolitt; omdanna eklogitt

20 Amfibolitt, lagdelt amfibolitt, amfibolrik gneis

21 Hornblende-glimmergneis

22 Marmor

23 Kvartsitt, nokre stader lagdelt

24 Glimmerskifer, granat-glimmerskifer, glimmergneis, granatamfibolitt; inneheld nokre stader linser og gangar av trondhjemitt og er nokre stader migmatittisk

Fig. 16 : Geological map of the Romsdal – Lesja areas (after Tveten et al., 1998). Eclogites from these areas are coarse-grained and relatively TiO_2-rich (3-4 % TiO_2), but unfortunately in most cases they are severely retrograded and much of the rutile has altered to ilmenite ± titanite. The microphotographs (2) and (3) are examples of eclogites from the Lesja area.

Fone

(3)

Ødegård

(4)

Laget

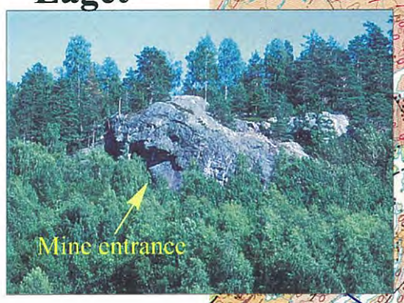

(2)

Bamblekomplekset

Gang- og dypbergarter og omdannede bergarter; mellomproterozoikum, eldre enn 1050 mill.år

- D — Diabasgang
- P — Pegmatittgang
- 33 — Granitt, noe forgneiset, stedvis hyperstenførende (charnockittisk)
- 34 — Mikrogranitt
- 35 — Granittisk øyegneis, grovkornet; omdannet granitt
- 36 — Granittisk øyegneis, stedvis hyperstenførende (charnockittisk)
- 37 — Noritt, leukonoritt
- 38 — Trondhjemitt, kvartsdioritt, forgneiset og foliert / Samme bergart mylonittisert
- 39 — Bergarter som inneholder hypersten, mesoperthitt, evt. granat (charnockittisk mineralogi). Punktregistrering
- 40 — Dioritttisk gneis, antatt omdannet dioritt, forgneiset og foliert
- 41 — Migmatitt, stedvis hyperstenførende (charnockittisk)
- 42 — Amfibolitt, stedvis hyperstenførende (charnockittisk)
- 43 — Albititt og tilhørende intrusjonsbreksje
- 44 — Gabbro, metagabbro, stedvis med koronatekstur
- 45 — Lys gabbro
- 46 U — Peridotitt / Peridotittpropp (U)
- 47 — Skapolitt-amfibolitt (Ødegårditt)

Omdannede sedimentære og vulkanske bergarter; mellomproterozoikum, 1700-1600 mill.år?

- 48 — Kvartsitt, kvartsrik gneis
- 49 — Konglomerat med boller av kvartsitt
- 50 n — Kvartsitt og kvartsglimmergneis i veksling, stedvis med sillimanitt og amfibol og med knollestruktur (n)
- 51 — Båndgneis, udifferensiert / Samme bergart mylonittisert
- 52 — Båndgneis, grafittførende
- 53 — Båndgneis med lyse og mørke lag i tett veksling; stedvis agglomeratiske ledd
- 54 — Kalkspatmarmor og skarn
- 55 — Båndgneis av mulig vulkansk opprinnelse / Samme bergart mylonittisert

Rutile deposit/occurrence

(1)

(5)

Fig. 17: Geological overview of the Bamble region (after Padget & Brekke 1996). The photographs are: (2) The entrance of the old rutile mine (prospect) in the cliff at Laget. (3) The entrance of the old rutile mine (prospect) in the forest at Fone. (4) Rutile-rich albitite (kragerøite) from within the old Lindvikkollen rutile mine. (5) Photograph of the old tailings from the apatite mining (1872-1945) at Ødegården. The rutile-bearing scaplolite – hornblende rock (called ødegårdite by Brøgger, 1934) is the country-rock to the phlogopite – enstatite veins that were mined for apatite.

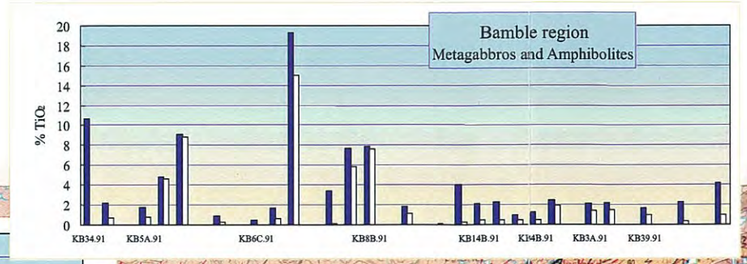

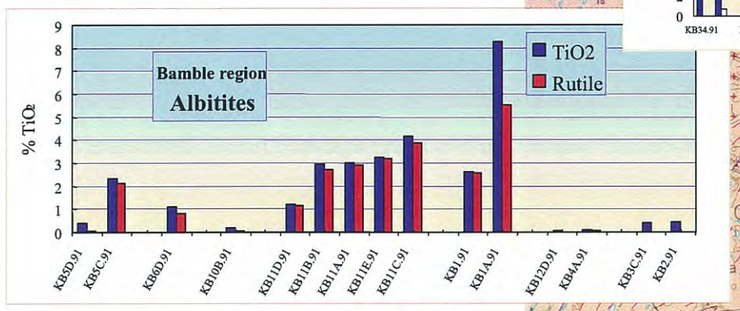

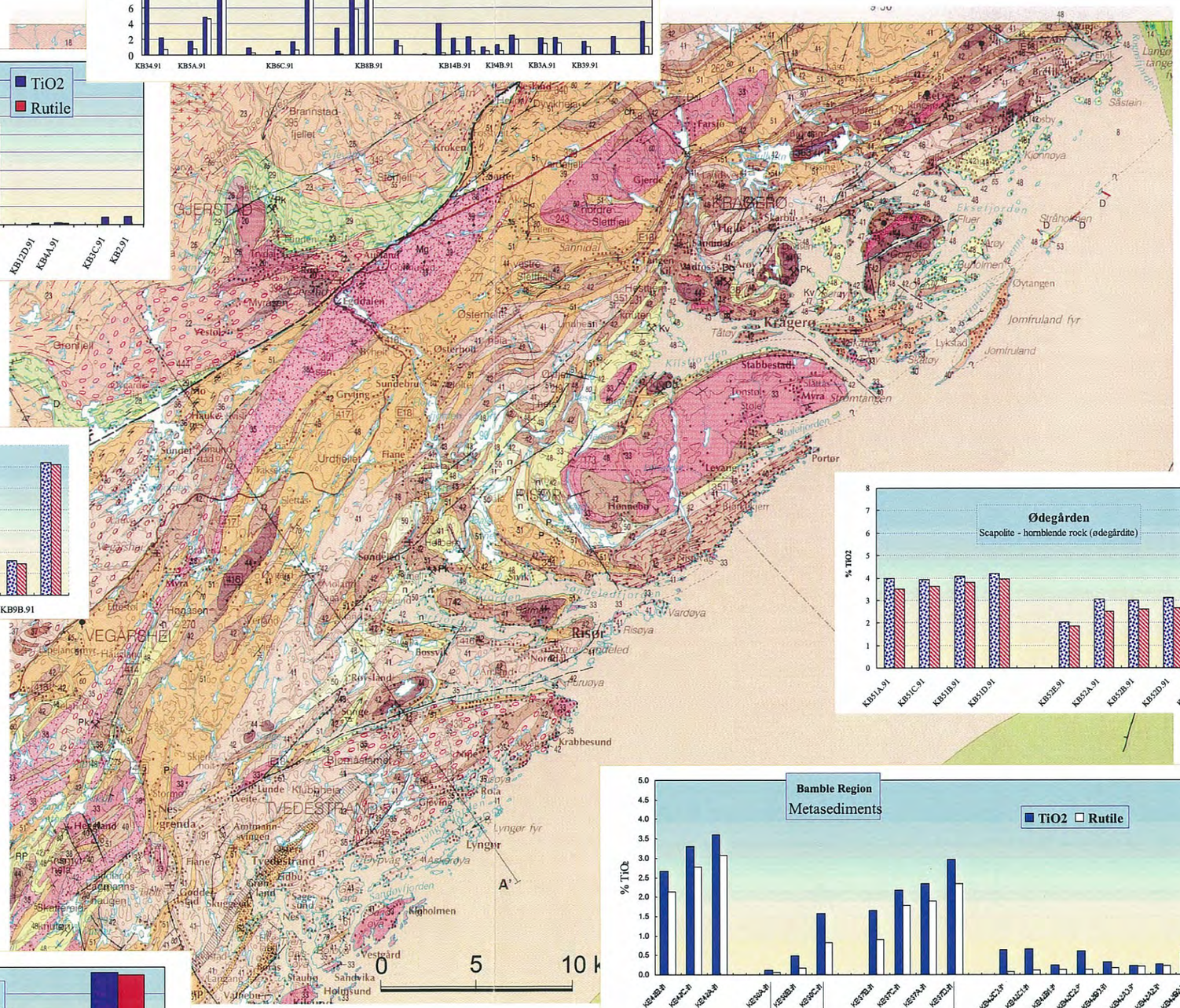

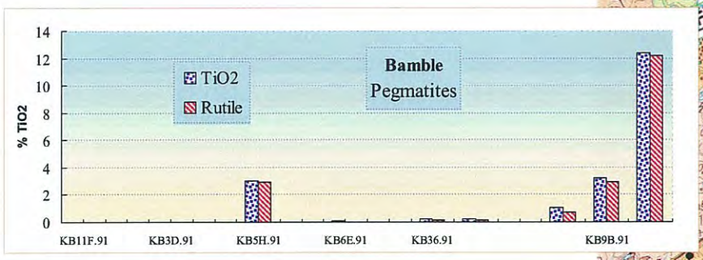

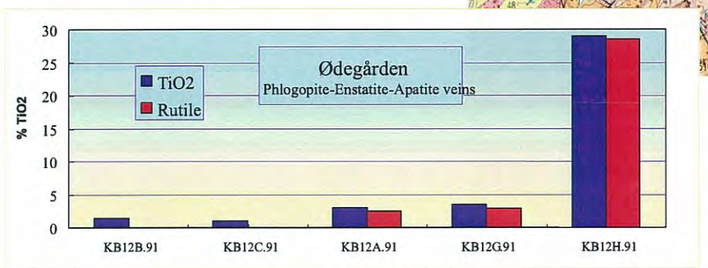

Fig. 18: Graphs showing Rutile/TiO_2-relations for various rutile-bearing rocks in the Bamble region. The graphs are based on analyses in Appendix 2.

Ødegården

(4)

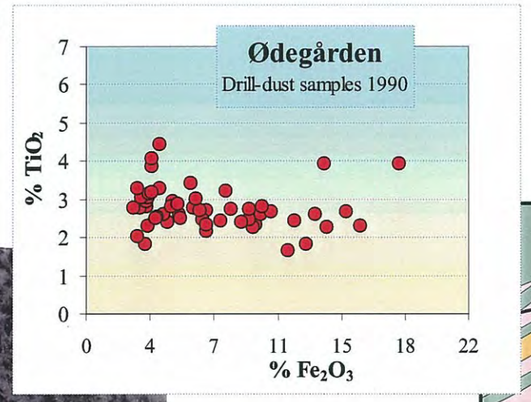

(6)

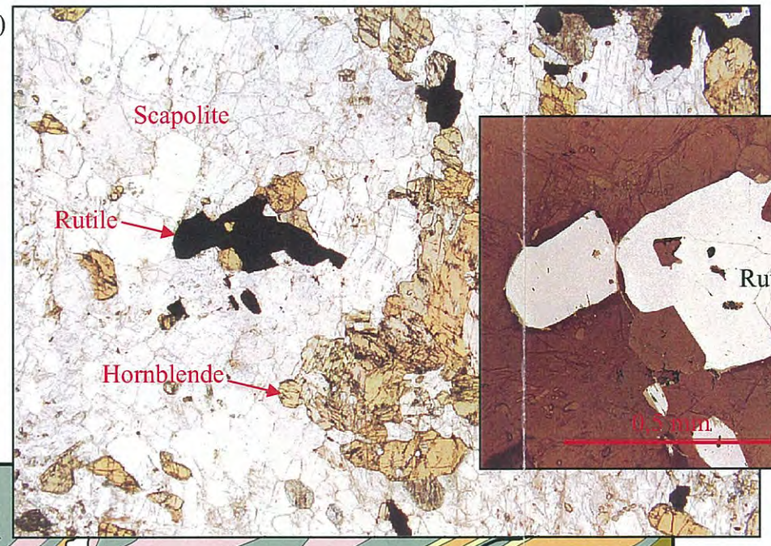

(7)

(8)

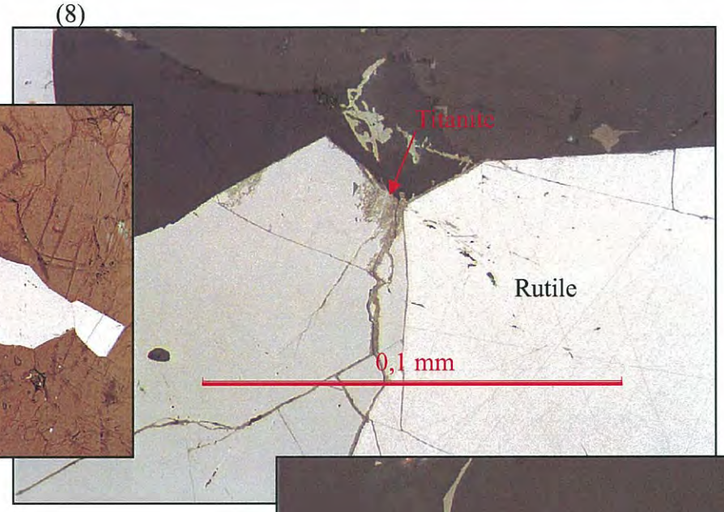

(9)

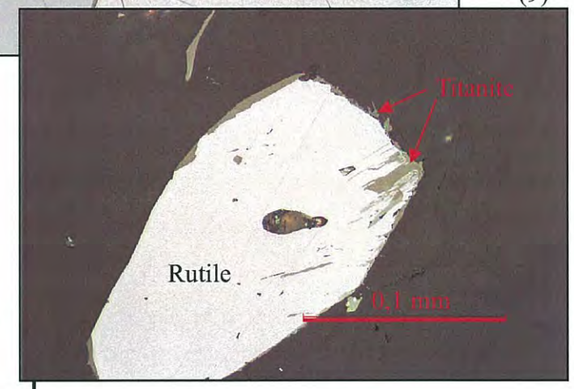

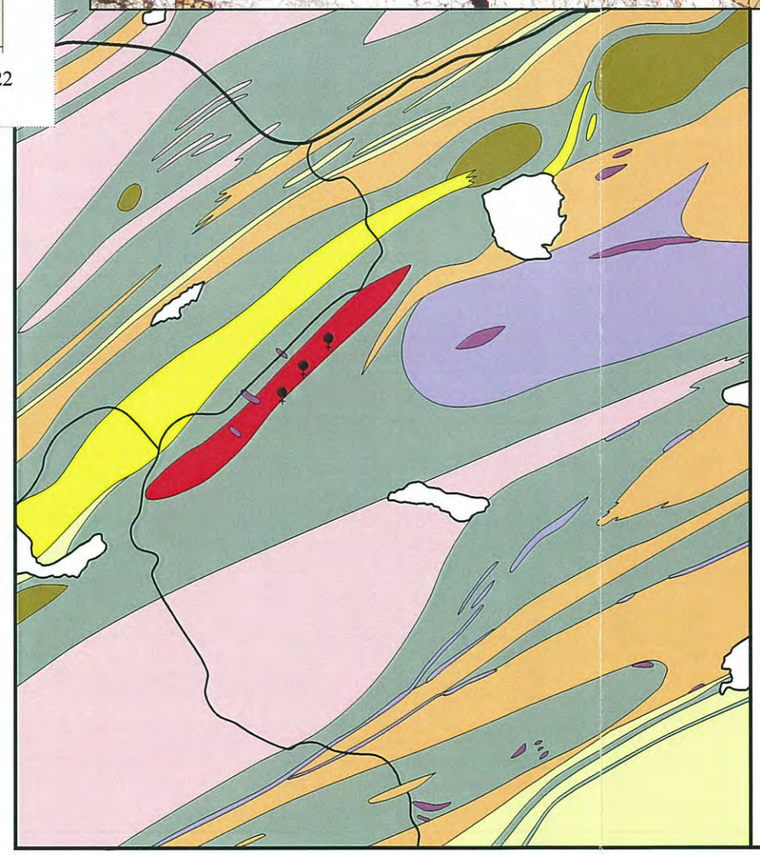

N

LEGEND

- GRANITIC GNEISSES
- ØDEGÅRDITE (scapolite+hornblende+apatite+rutile)
- ALBITITE
- AMPHIBOLITE
- BASIC INTRUSIONS
- Quartz+plagioclase+biotite schists
- Cordierite+phlogopite schists
- QUARTZITE
- PEGMATITE
- Apatite mine
- Road

From manus map
M.J. Ryan 1964-66.
NGU archive.

1 km

(1)

(2)

3,5 cm

(3)

3,5 cm

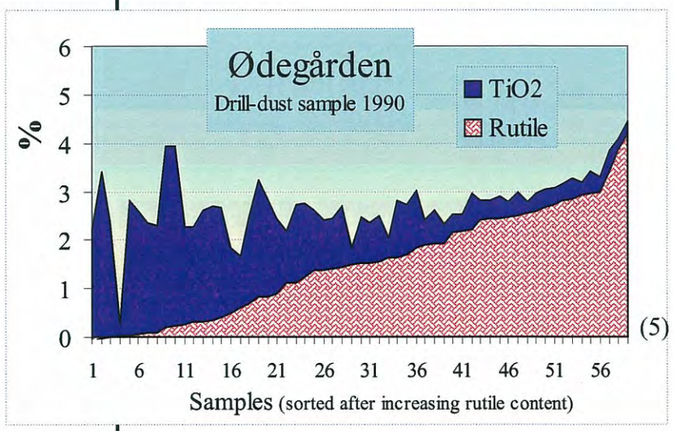

(5)

Fig. 19: The Ødegården rutile deposit, Bamble region. The geological map (1) is after Ryan (1964-66). The core samples (2) and (3) are showing two variations of scapolitised gabbro (ødegårdite) with the gabbroic texture well-preserved. The graphs in figures (4) and (5) are of drilldust surface samples, with the analytical data given in Appendix 2. The occurence of rutile in the rock is shown by the microphotographs (6) to (9).

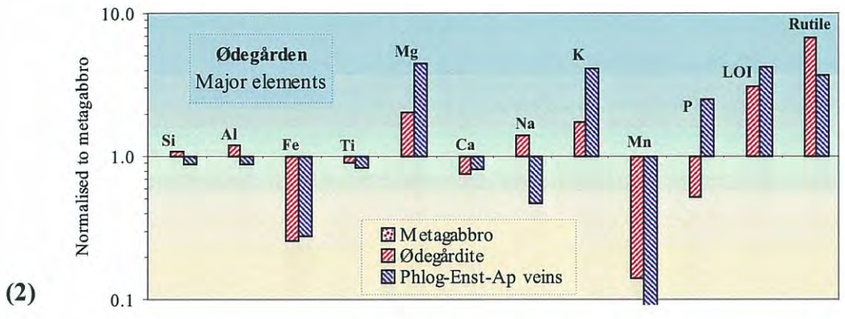

(2)

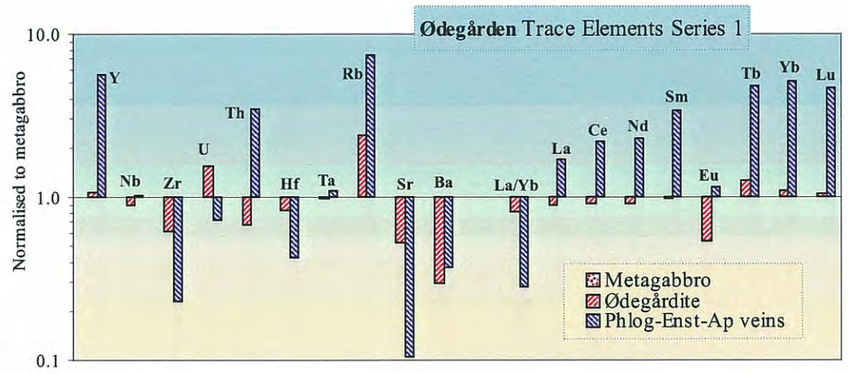

(2)

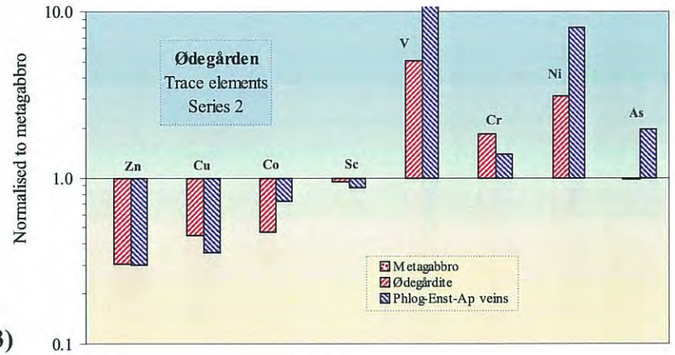

(3)

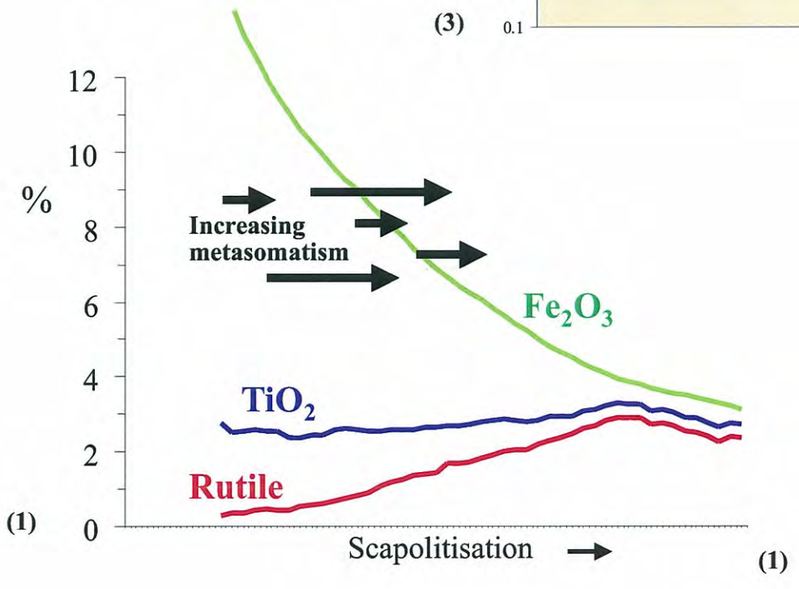

(1) (1)

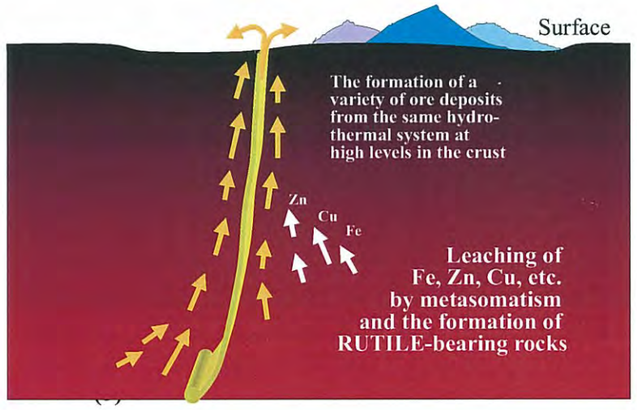

(2)

Fig. 20: Major- and trace element relations in metasomatic rocks from the Ødegården rutile deposit, Bamble region. Figure 1 is a line-plot showing the variations in rutile-, TiO_2- and Fe_2O_3 contents with increasing degree of metasomatism (scapolitisation in this case). See the analytical data in Table 3. The figures 2, 3 and 4 are showing the relative variations in major- and trace elements between the 3 major rock-types at Ødegården. Metagabbro is an amphibolitic gabbroic rock that has not suffered significant metasomatism. Ødegårdite is a rutile-bearing scapolite – hornblende rock, representing the metasomatised variety of the metagabbro. Gradual transitions between ødegårdite and metagabbro are common. The phlogopite – enstatite - apatite rock occur as dykes or veins intruding into the ødegårdite, thus representing a later magmatic/hydrothermal phase. Figures 2, 3 and 4 are based on the analytical data given in Table 4. Figure 5 is a visualisation of a geological model in which hydrothermal fluids are leaching metals such as Fe, Zn and Cu from rocks in the lower crust, leaving most of the titanium behind as rutile. In this process large amounts of metals are transported to higher levels in the crust to be precipitated and concentrated into various types of hydrothermal, epigenetic ore deposits.

(5)

(4)

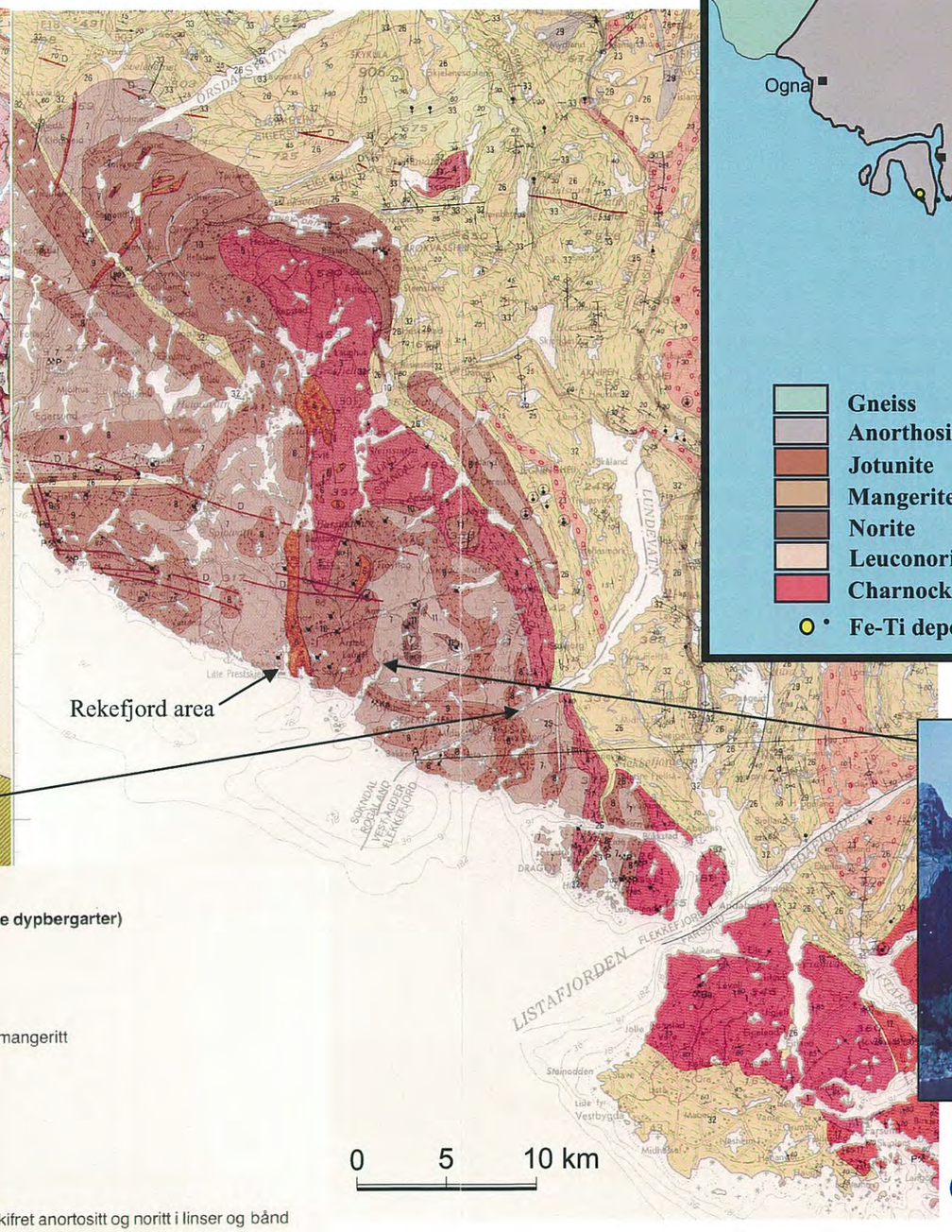

(1)

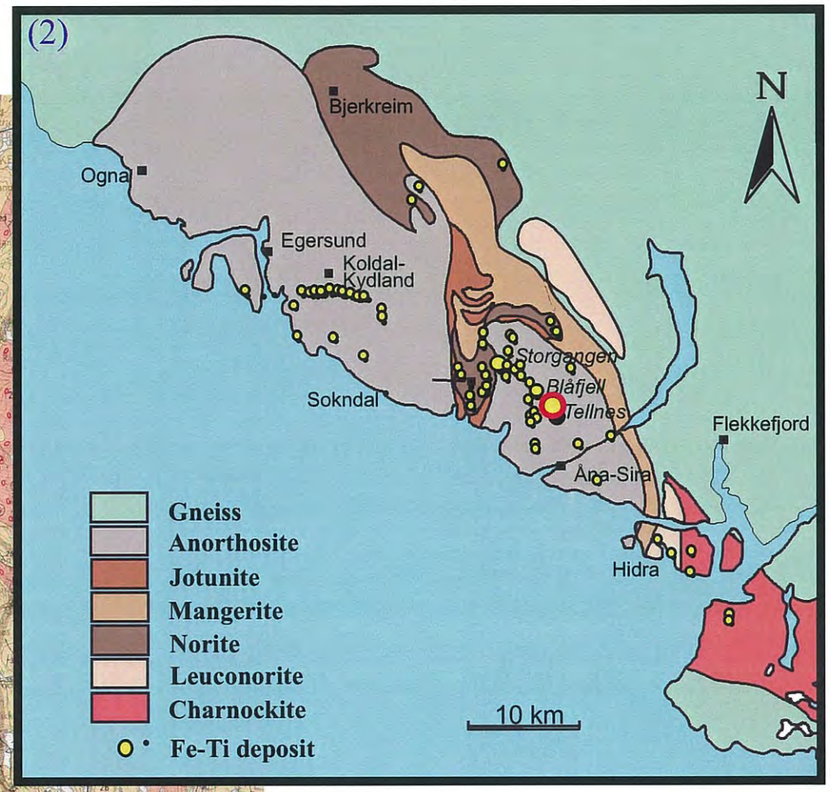

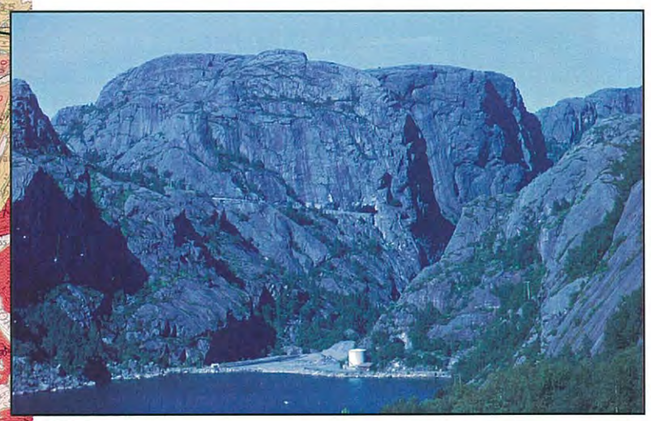

(3)

Bergarter av prekambrisk alder

Egersundkomplekset (anortosittiske–charnockittiske dypbergarter)

1	Charnockitt (ortopyroxen-granitt)
2	Charnockitt (ortopyroxengranitt) foliert
3	Pyroxen-kvartsmonzonitt, stedvis fayalittførende, kvartsmangeritt
4	Pyroxen-kvartsmonzonitt, kvartsmangeritt-, foliert
5	Pyroxenmonzonitt, mangeritt
6	Monzonoritt (jotunitt)
7	Anortositt
8 9	Anortositt, leuconoritt og noritt med linser av noritt / Forskifret anortositt og noritt i linser og bånd
10	Leuconoritt
11 12	Noritt/gabbronoritt (hyperitt), gabbro

Fig. 21: (1) Geological map of the Rogaland anorthosite province from the geological map-sheets (1:250000) Stavanger (Jorde et al. 1995) and Mandal (Falkum 1982), and (2) a simplified geological map of the same province. The photograph (3) is from a landscape at Jøssingfjord, photograph (4) is showing alteration of the primary anorthosite (dark) to secondary white anorthosite along fractures, while photograph (5) is from the quarrying of white anorthosite for aggregate at Hellevik.

Altered anorthosite from the Rekefjord area, Rogaland Anorthosite Province.

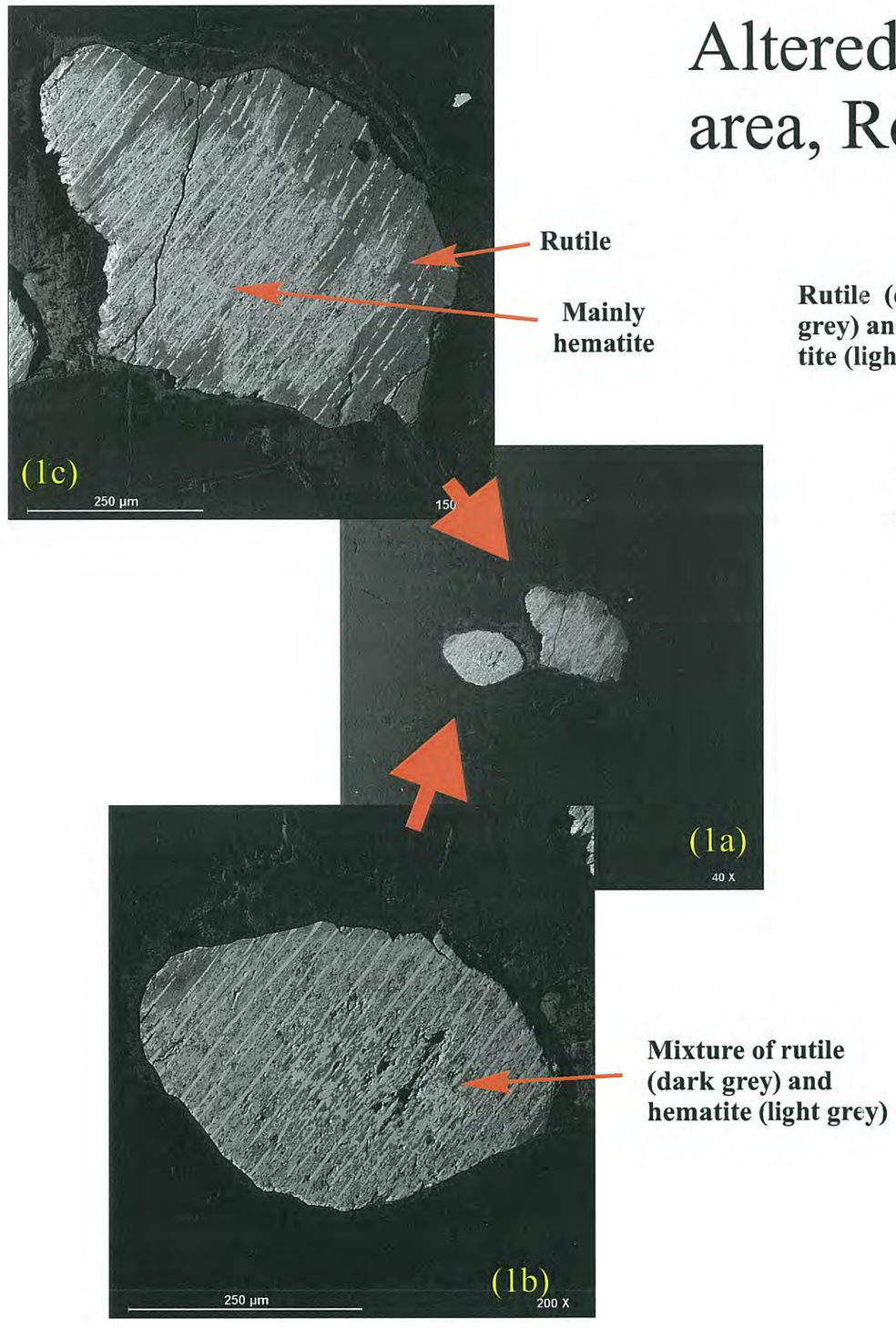

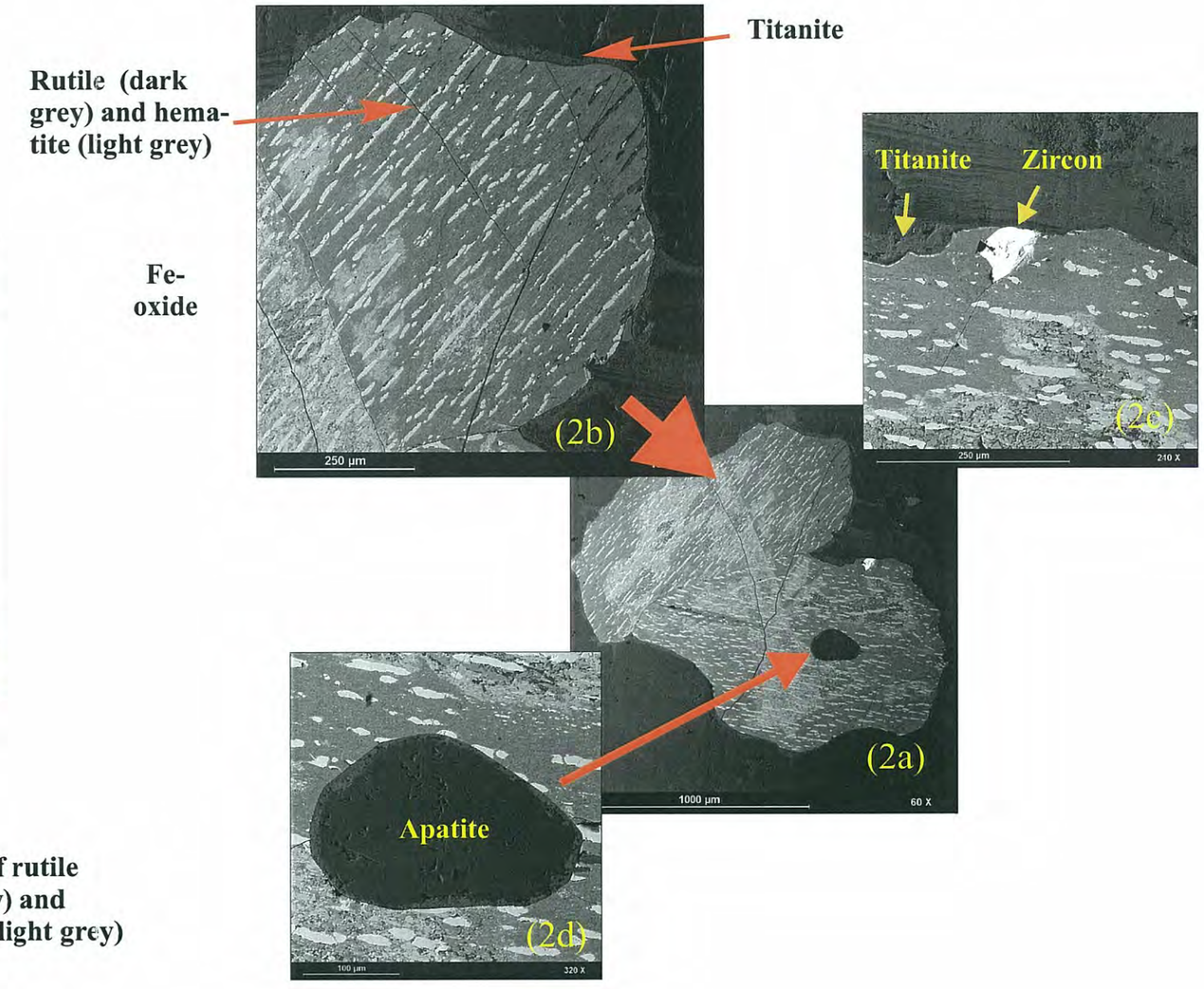

Fig. 22: SEM back-scattered images showing Fe-Ti oxides and titanite in altered anorthosite from the Rekefjord area. Unpublished data from Lars Petter Nilsson (NGU) .The major part of the oxide grains, such as in Fig. (2b)consists of rutile (dark grey) closely associated with chlorite (not distinguishable from rutile in these images).The light grey lamellae is Fe-oxide, probably hematite. The major grains are rimmed by titanite. Presumably rutile with hematite exsolutions, was formed from ilmenite during an early stage of the hydrothermal alteration period, followed by the formation of titanite rims at a later stage.

Fe-Ti oxides and titanite in altered anorthosite from the Rekefjord area, Rogaland anorthosite province

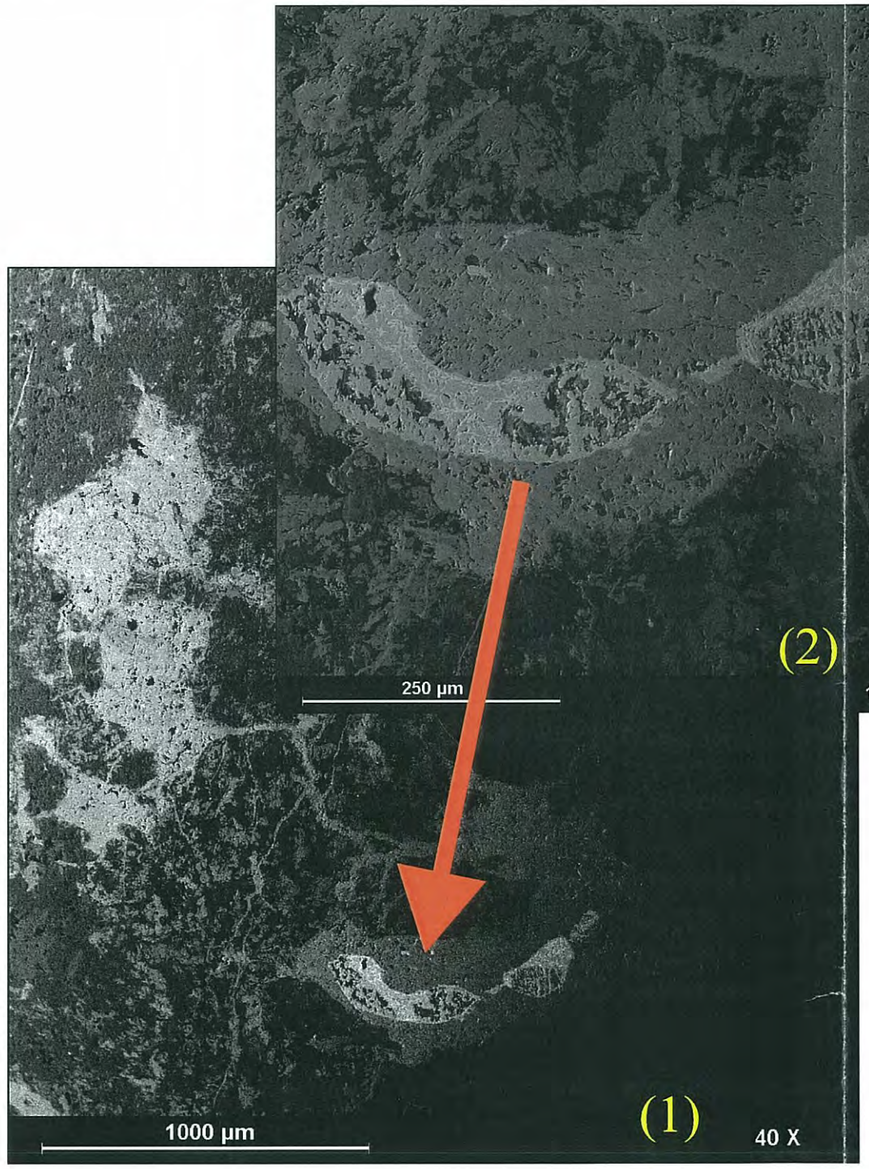

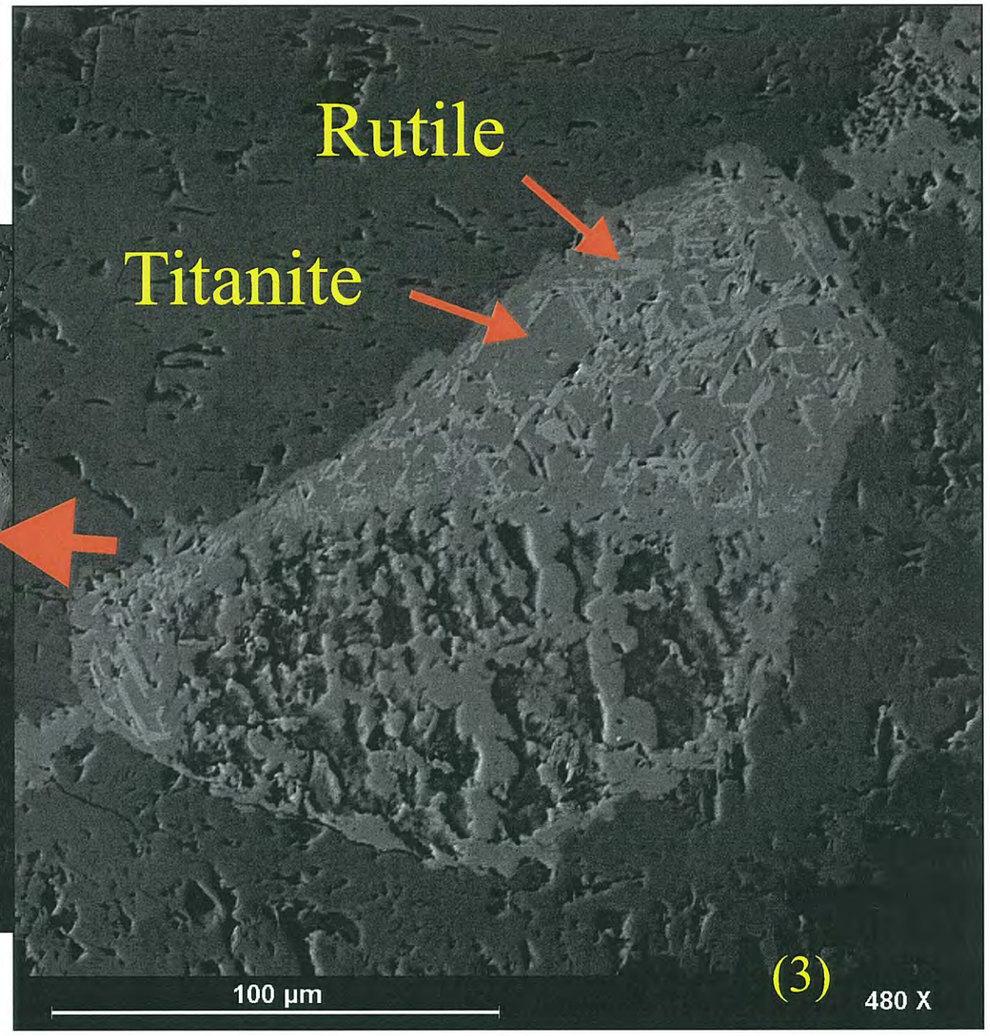

Fig. 23: SEM backscattered images of altered anorthosite from the Rekefjord are. Fig (1) shows aggregates(light grey) of altered Fe-Ti oxides from the original anorthosite. The aggregate at the lower part of Fig. (1) is shown in more detail in Fig. (2), while Fig. (3) shows an enlarged portion of the same aggregate The rutile occur as numerous elongate grains surrounded by titanite. Although the detailed relations are unclear, the general impression is that ilmenite w as altered to rutile at an early hydrothermal stage followed by the alteration of rutile to titanite.

ENGEBØFJELLET

(1)

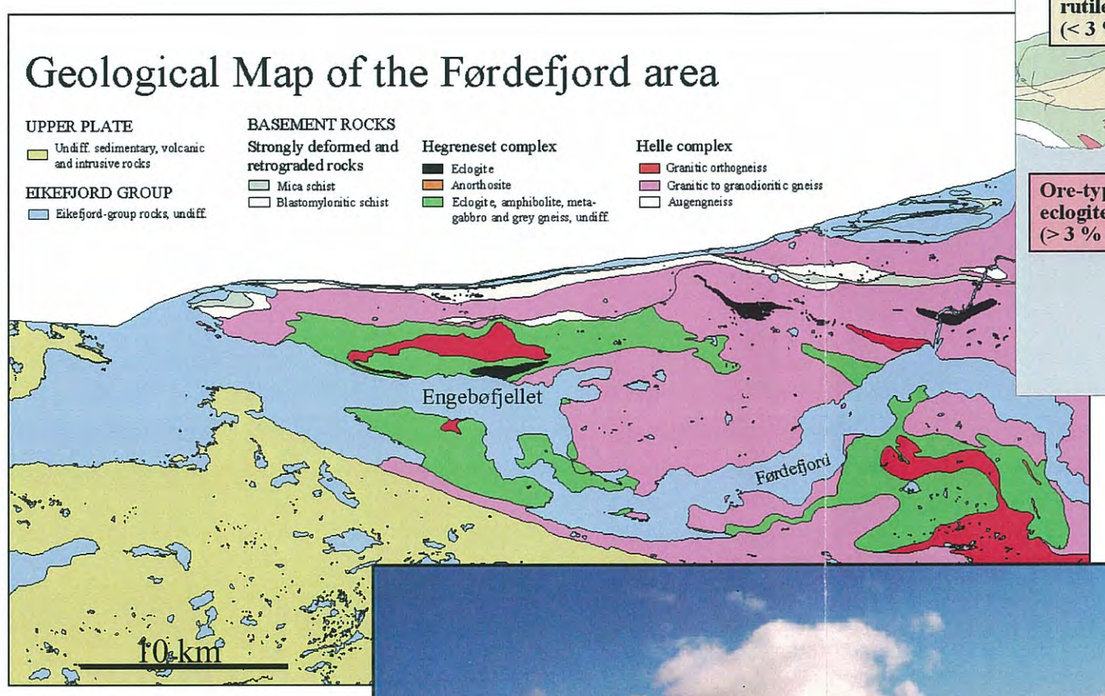

(2)

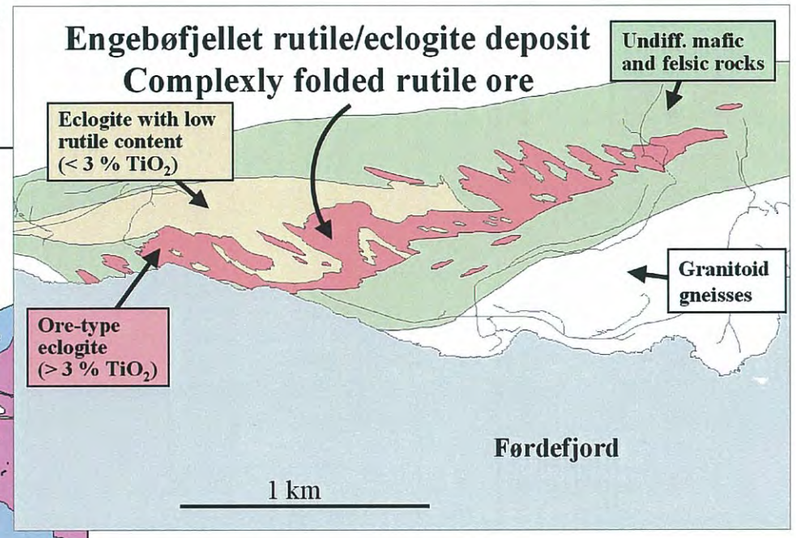

(3)

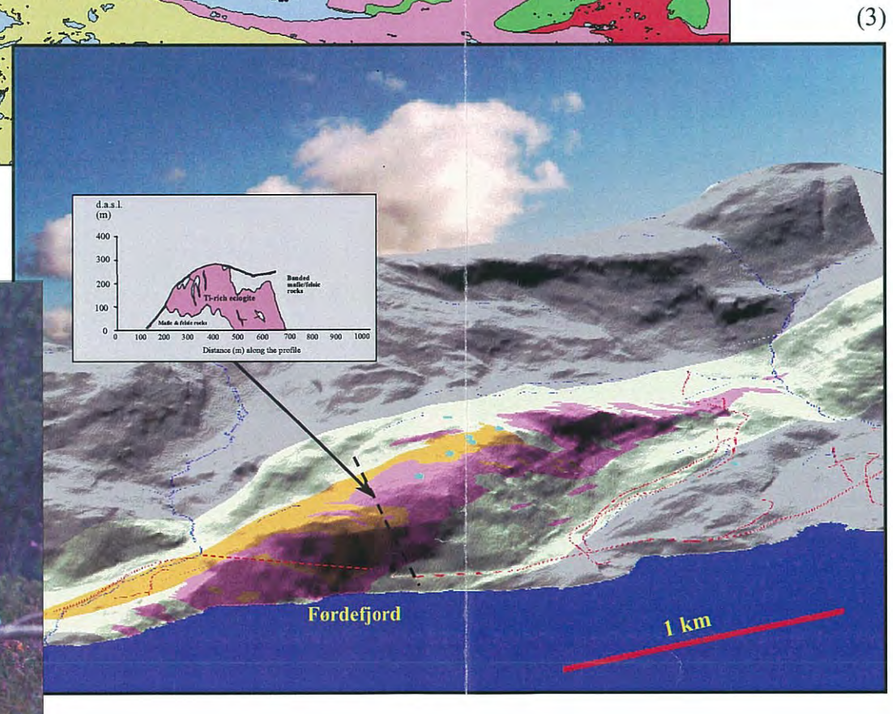

(4)

Fig. 24: Overview geological maps, Engebøfjellet eclogite. Figure (1) is a simplified geological map of the Førdefjord region and Figure (2) a geological map of the Engebøfjellet eclogite deposit. Figure (3) is a terrain model of Engebøfjellet that shows the surface exposure of the ore-type eclogite (also called ferro-eclogite; > 3 % TiO_2) in red and other eclogite varieties (leuco- and transitional eclogite; < 3 % TiO_2) in yellow. The photograph (4) is of the two senior geologists Magnus Garson (consultant for DuPont) and Roger McLimans (DuPont's chief geologist) who, first of all, have been the driving force in DuPont/ Conoco's rutile/eclogite investigation in Norway.

ENGEBØFJELLET

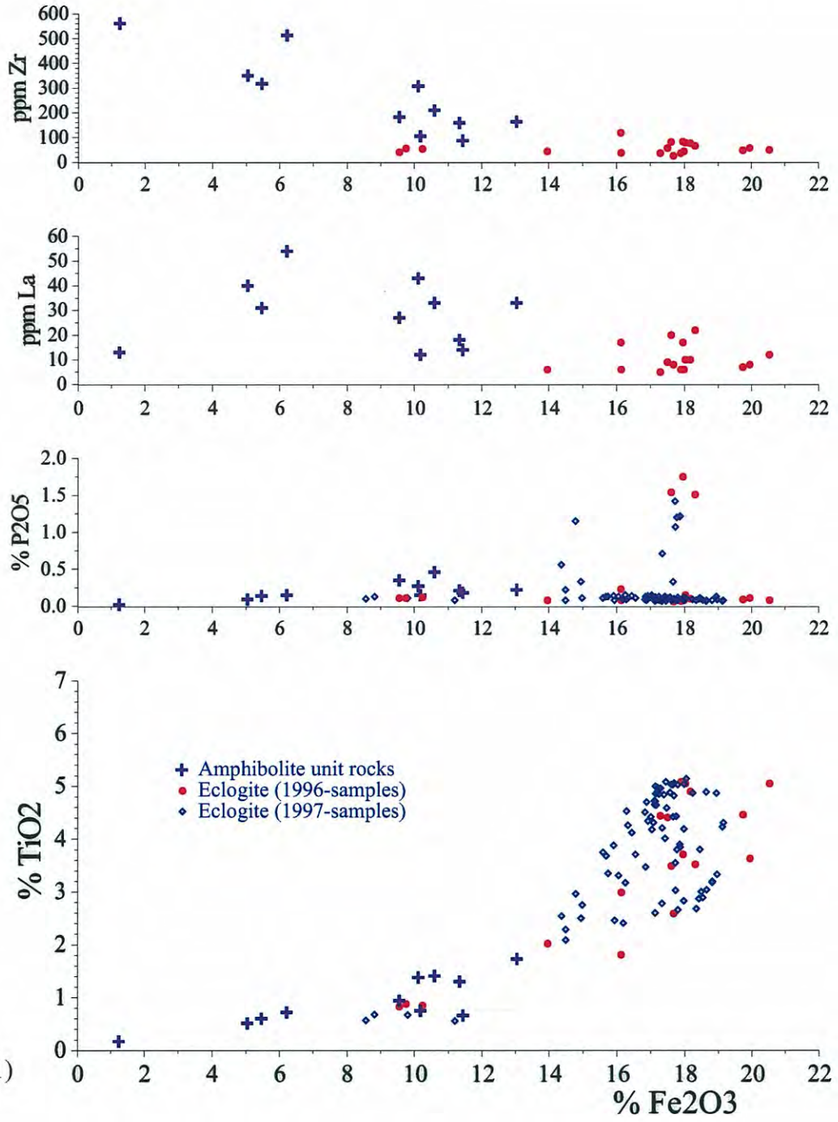

TiO_2, P_2O_5, La and Zr vs. Fe_2O_3 in core-sections.
The "Amphibolite unit" are mixed mafic- and felsic rocks representing the country-rocks to the Engebøfjellet eclogite. These are distinctly different in character and chemical composition compared to the other eclogite varieties that are plotted, which belong to the main eclogite body.

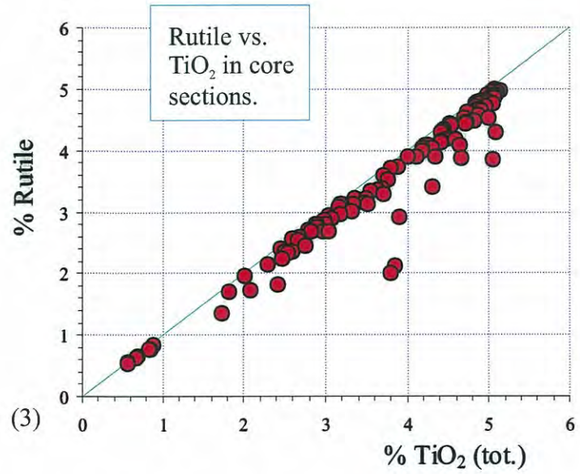

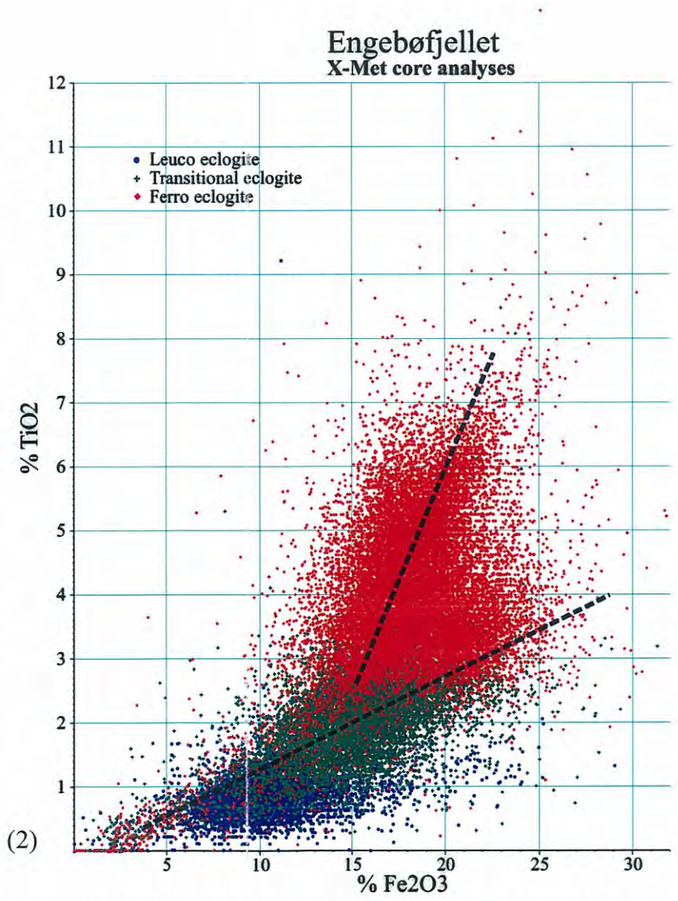

Fe_2O_3 - TiO_2 plot of approx. 50.000 point-analyses directly on drill-cores by the X-Met portable XRF.

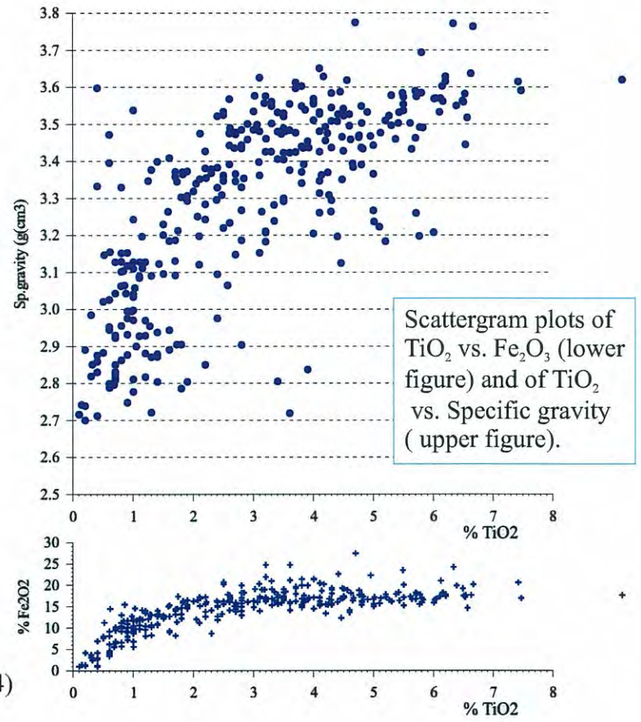

Scattergram plots of TiO_2 vs. Fe_2O_3 (lower figure) and of TiO_2 vs. Specific gravity (upper figure).

Fig. 25: Miscellaneous analyses, Engebøfjellet eclogite. (1) X-Y plots of Fe_2O_3 vs. TiO_2, P_2O_5, La and Zr based on XRF-analyses of core-samples. (2) Fe_2O_3 – TiO_2 plot of point-analyses done directly on eclogite cores by the X-Met portable XRF. (3) Rutile vs. TiO_2 in core-sections. (4) Scattergram plot showing the relation between TiO_2 and specific gravity and between TiO_2 and Fe_2O_3 in the same core samples.

ENGEBØFJELLET

(1)

(2)

(3)

(4)

(5)

(6)

(7)

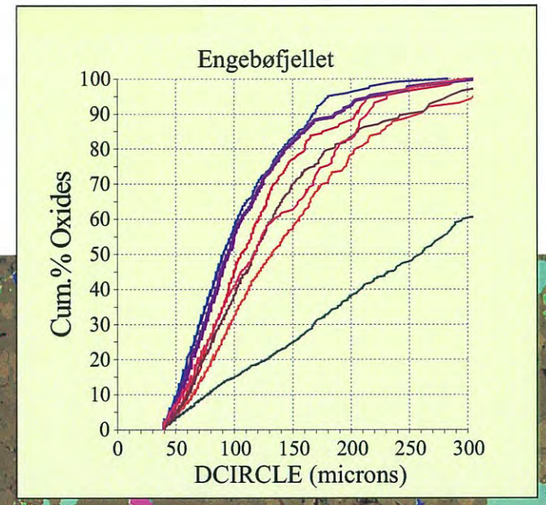

(8)

Fig. 26: Microphotographs of Engebøfjellet eclogite. (1) Thin-section E3/127.3 (transmitted light) showing a characteristic pattern of fractures along which fluids have had access under amphibolite facies metamorphic conditions leading to retrograde alteration of eclogite along these fracture to amphibolite. The dominant minerals outside these fractures are garnet and omphacitic clinopyroxene. Rutile is see n as dark brown to black grains. Some of the large opaque grains are pyrite. (2) and (3) are microphotograph showing the same section of thin-section E3/127.3 in transmitted and reflected light, respectively, while (4) and (5) shows rutile details at high magnification. (6) is an example of rutile (reflected light) that has be en altered to ilmenite and titanite along a retrograde fracture similar to the one in Fig. (1). The variation in grain-size distribution of minerals with high reflectivity, i.e. rutile, ilmenite and pyrite, between some thin-sections from Engebøfjellet is shown in Fig. (7). In Fig. (8) various oxide grain-size intervals (0.05 mm, 0.50-0.10 mm, 0.10-0.15 mm. 0.15-0.20 mm, 0.20-0.25 mm and > 0.25 mm) in thin-section E4/120.9 are shown by different colour.

Engebøfjellet

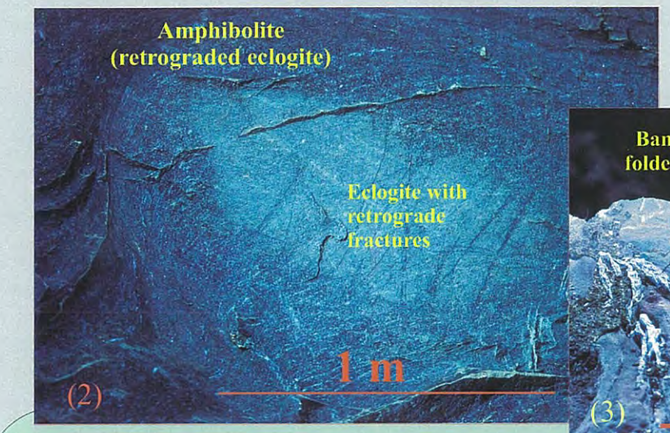

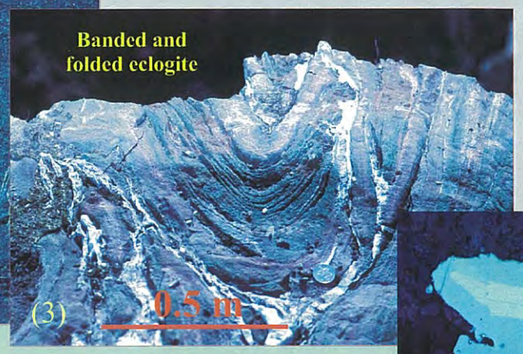

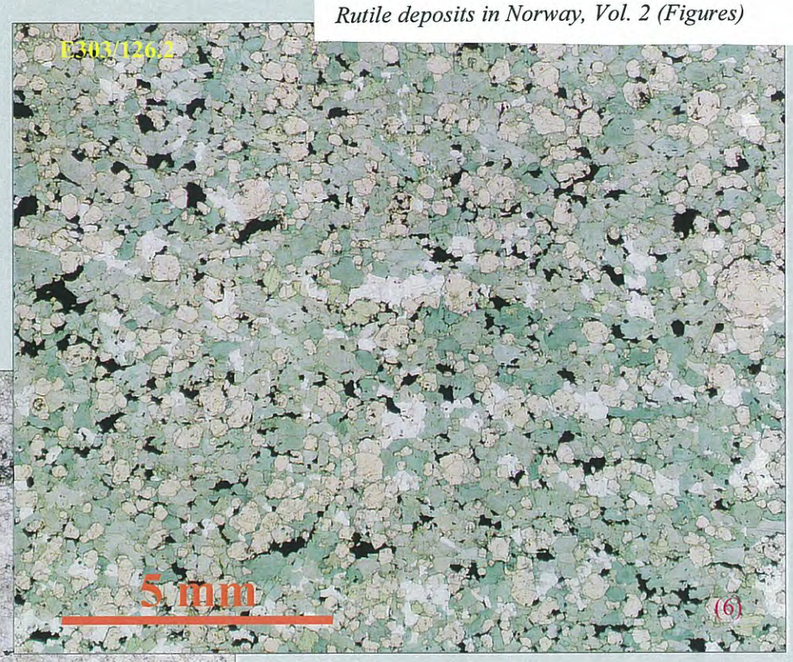

XRD

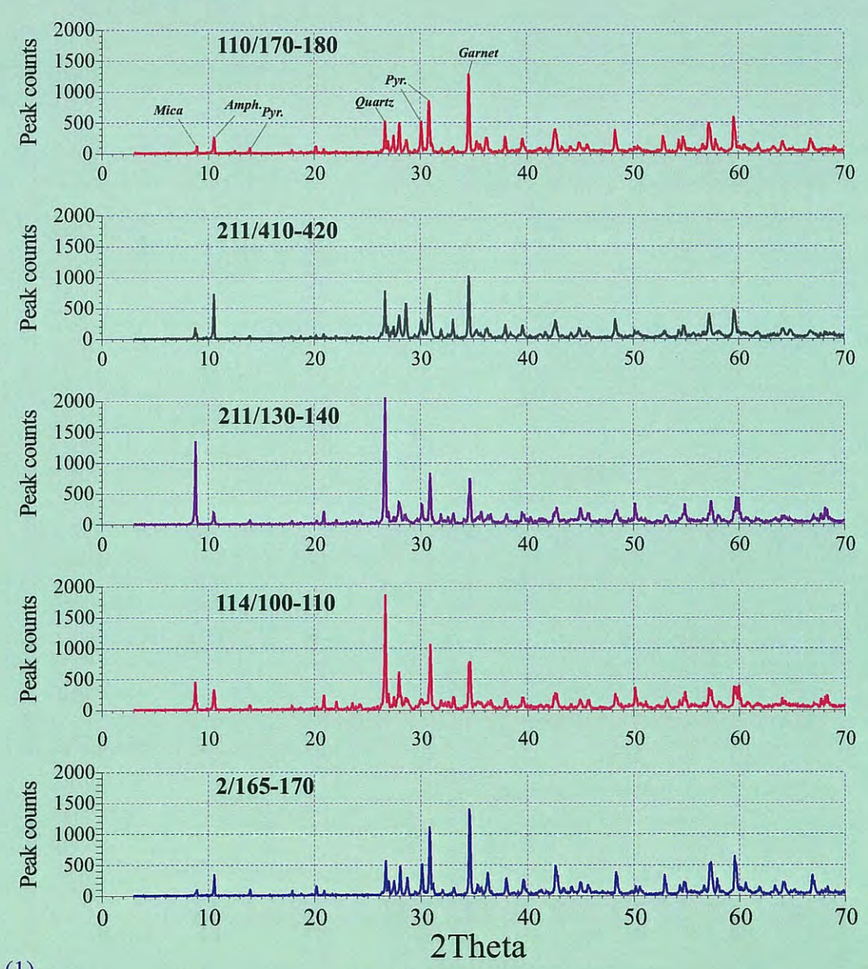

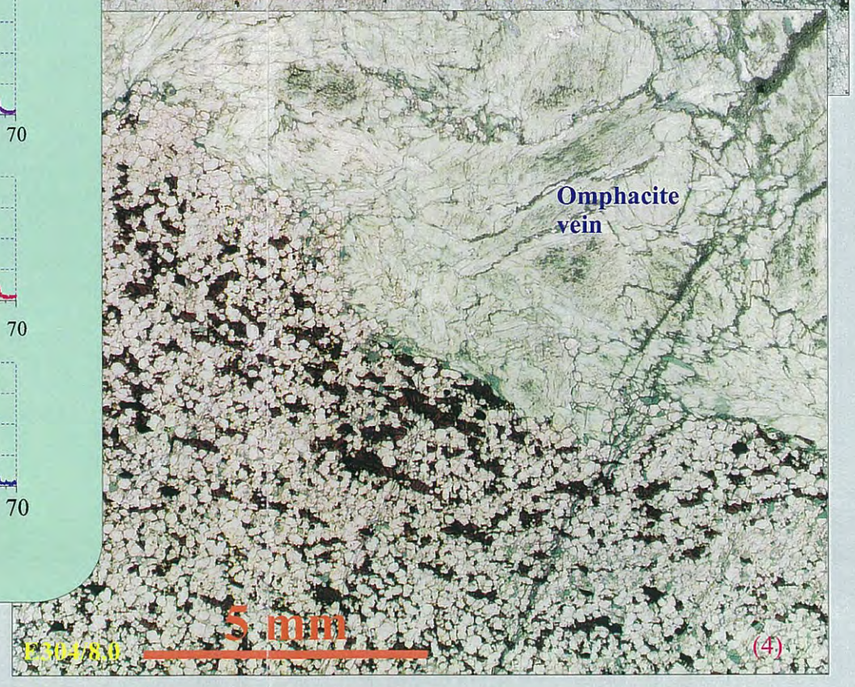

Fig. 27: XRD-analyses of pulverised splits of Engebøfjellet cores (Part I). Large parts of the Engebøfjell eclogite are very heterogeneous in modal composition in cm-dm-m scale due to its complex metamorphic and deformational evolution. The purpose of this presentation is (a) to illustrate some of the mineralogical heterogeneity of the eclogite rocks and (b) suggest that XRD might be a convenient method to quantify the mineralogical variations.

Figure (1) shows a selection of XRD-patterns in which variations in *average modal* composition in 5 and 10m core sections are shown by differences in the distribution and size of the individual peaks. Figure (2) is a field-photo of eclogite that is altered to amphibolite along fractures in the core of the exposure, surrounded by completely amphibolitised eclogite. Figure (3) is an example of banded and folded eclogite with quartz-veins. Figure (4) is a microphotograph (thin-section E304/8.0) showing rutile-rich, fine-grained garnet-omphacite eclogite in contact with an omphacite vein. Figure (5) is a microphotograph of fine-grained garnet- and omphacite rich eclogite with distinct retrogression (amphibolitisation) along a fracture similar to the fractures in the centre of Figure (2). Figure (6) is a microphotograph giving an example of a garnet- and amphibole-rich eclogite. Figure (7) is a microphotograph (reflected light) of rutile from a retrograde fracture in eclogite, similar to the fracture in (5), which has been altered to ilmenite and then to titanite.

ENGEBØFJELLET

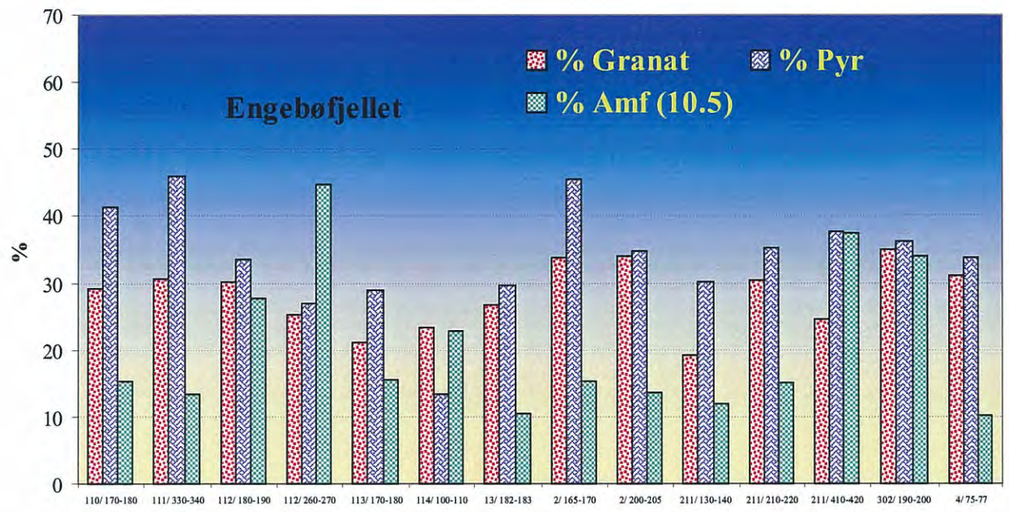

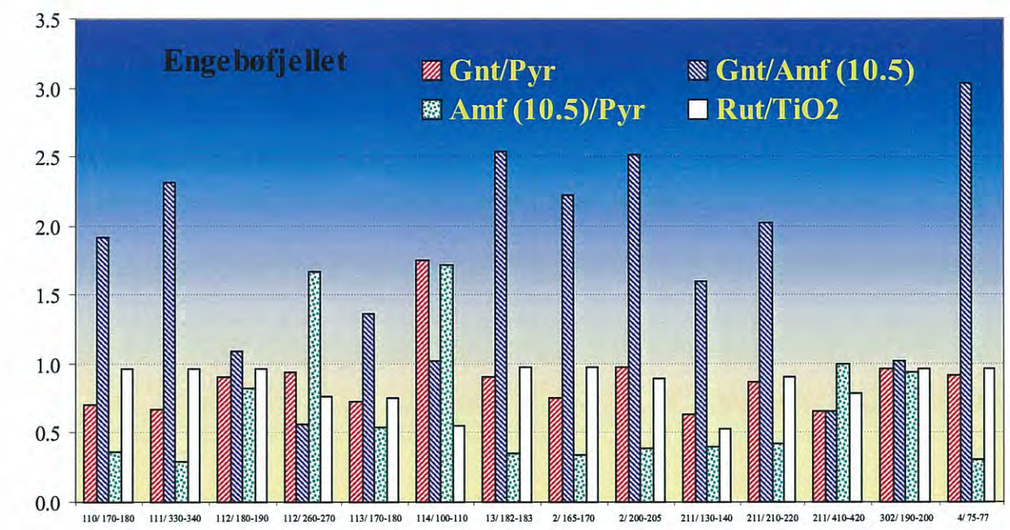

Tabell 1: Beregnet konsentrasjoner basert på kalibreringermodell med absorpsjonskoeffisienter.
For amfibol er det beregnet konsentrasjon ved bruk av to ulike analyselinjer, hhv. 28.7°2q og 10.5°2q

Prøvenr	Prøve id	(1) % Granat	(2) % Pyr	(3) % Amf. (28.7)	Sum (1)+(2) +(3)	(4) % Amf (10.5)	*Sum (1)+(2) +(4)*	(1)/(2) Gnt/Pyr	(1)/(4) Gnt/Amf	(4)/(2) Amf/Pyr
110/170-180	1997.0298 pr. 10	29.21	41.29	7.44	77.94	15.25	*85.74*	0.71	1.92	0.37
111/330-340	1997.0342 pr. 3	30.65	45.89	9.32	85.86	13.26	*89.80*	0.67	2.31	0.29
112/180-190	1997.0342 pr. 4	30.15	33.44	14.23	77.82	27.62	*91.21*	0.90	1.09	0.83
112/260-270	1997.0342 pr. 5	25.27	26.89	26.26	78.42	44.84	*96.99*	0.94	0.56	1.67
113/170-180	1997.0342 pr. 7	21.13	28.91	3.73	53.76	15.57	*65.60*	0.73	1.36	0.54
114/100-110	1997.0342 pr. 31	23.29	13.34	4.65	41.28	22.86	*59.49*	1.75	1.02	1.71
13/182-183	1997.0086 pr. 4	26.72	29.72	5.17	61.62	10.56	*67.00*	0.90	2.53	0.36
2/165-170	1996.0046 pr. 9	33.88	45.33	10.81	90.02	15.23	*94.44*	0.75	2.22	0.34
2/200-205	1996.0046 pr. 10	34.09	34.87	4.95	73.91	13.56	*82.52*	0.98	2.51	0.39
211/130-140	1997.0342 pr. 9	19.08	30.13	5.50	54.72	11.98	*61.19*	0.63	1.59	0.40
211/210-220	1997.0342 pr. 10	30.39	35.15	10.78	76.32	15.06	*80.60*	0.86	2.02	0.43
211/410-420	1997.0342 pr. 12	24.58	37.67	24.78	87.03	37.41	*99.66*	0.65	0.66	0.99
302/190-200	1997.0342 pr. 23	34.91	36.22	20.49	91.62	34.14	*105.27*	0.96	1.02	0.94
4/75-77	1996.0046 pr. 19	31.04	33.77	8.26	73.07	10.25	*75.07*	0.92	3.03	0.30

Tabell 2: XRF-hovedelement analyser og magnetisk susceptibilitet (SI-enheter) av borkjernene.

Prøvenr	Prøve id	SiO_2	Al_2O_3	Fe_2O_3	TiO_2	MgO	CaO	Na_2O	K_2O	MnO	P_2O_5	LOI	Sum	Rutil
110/170-180	1997.0298 pr. 10	43.95	12.66	17.26	4.95	5.99	10.12	2.46	0.33	0.20	0.09	0.07	98.07	4.77
111/330-340	1997.0342 pr. 3	46.07	13.78	16.33	4.26	5.31	9.19	2.74	0.47	0.19	0.11	0.54	99.00	4.09
112/180-190	1997.0342 pr. 4	44.11	13.22	17.20	4.97	5.99	9.87	2.38	0.38	0.20	0.09	0.46	98.87	4.81
112/260-270	1997.0342 pr. 5	46.78	14.09	16.19	2.41	5.89	9.60	2.55	0.40	0.16	0.09	0.60	98.78	1.83
113/170-180	1997.0342 pr. 7	47.44	11.66	17.86	3.90	4.04	8.32	2.70	0.88	0.24	1.21	0.22	98.48	2.92
114/100-110	1997.0342 pr. 31	47.27	11.68	17.87	3.85	4.01	8.19	2.88	0.51	0.21	1.22	0.74	98.42	2.13
13/182-183	1997.0086 pr. 4	43.40	13.72	17.44	5.10	5.26	9.85	2.05	0.45	0.20	0.07	0.72	98.26	4.95
2/165-170	1996.0046 pr. 9	44.56	13.15	18.02	5.05	5.22	9.76	2.30	0.40	0.21	0.15	0.01	98.83	4.90
2/200-205	1996.0046 pr. 10	42.59	13.38	18.31	3.52	4.30	9.50	2.23	0.52	0.25	1.51	0.10	96.22	3.14
211/130-140	1997.0342 pr. 9	47.56	11.49	17.77	3.80	4.00	7.89	2.44	1.05	0.25	1.20	0.73	98.19	2.02
211/210-220	1997.0342 pr. 10	44.84	13.64	16.92	4.34	5.26	9.63	2.64	0.38	0.21	0.14	0.30	98.30	3.90
211/410-420	1997.0342 pr. 12	44.34	13.29	17.08	4.31	6.06	9.88	2.35	0.43	0.21	0.12	0.65	98.71	3.40
302/190-200	1997.0342 pr. 23	43.53	12.96	17.69	5.06	6.31	10.19	2.29	0.21	0.21	0.10	0.22	98.76	4.84
4/75-77	1996.0046 pr. 19	43.12	13.99	17.98	5.09	5.36	9.81	2.11	0.43	0.21	0.08	0.95	99.13	4.91

Fig. 28: Quantitative XRD-analyses, Engebøfjellet (Part II).
Concentrations of the main minerals garnet, omphacitic clinopyroxene and amphibole in Engebøfjellet core-samples.

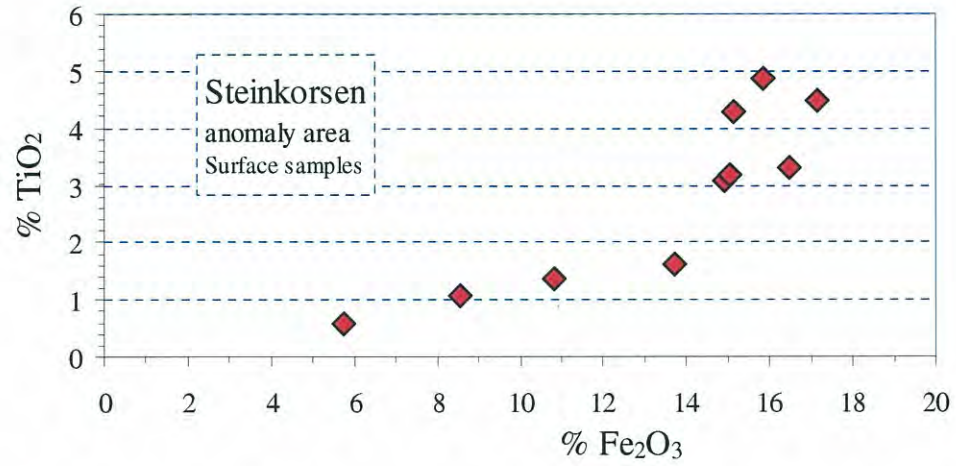

Fig. 29: Fe_2O_3 – TiO_2 scattergram plot showing the TiO_2 and Fe_2O_3 content in chip-samples (average values) from the Steinkorsen anomaly area. The analytical data are given in Table 4.

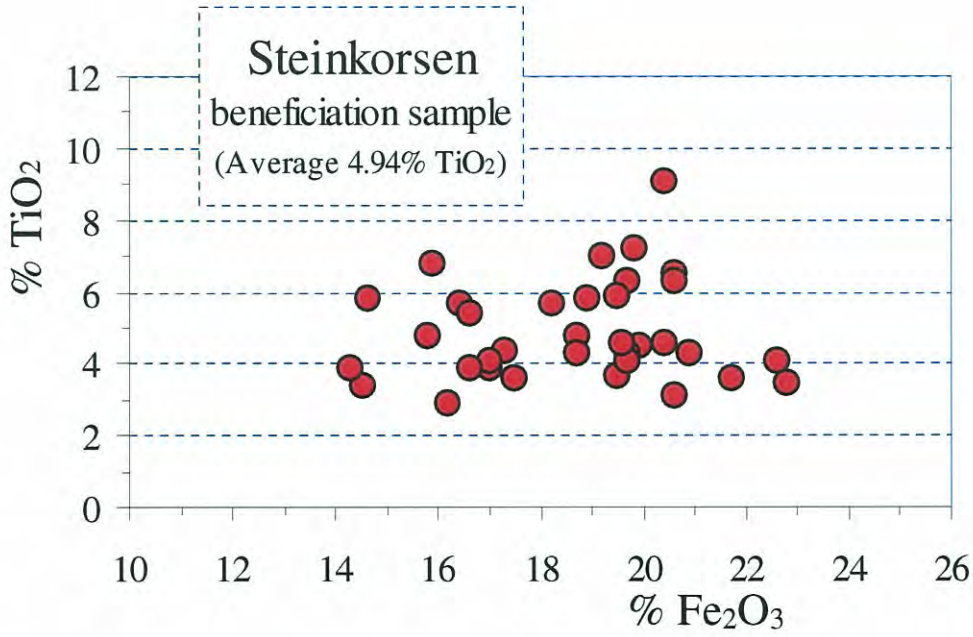

Fig. 30: Fe_2O_3 – TiO_2 scattergram plot showing the TiO_2 and Fe_2O_3 content in sub-samples from a large (30-40 kg) sample at the Steinkorsen locality K148.99 taken for further investigation by Rio Tinto Iron & Titanium. Each analytical value represent one surface analyses done by the X-Met portable XRF, and is not representative for the respective sub-sample, since the rutile in the rock is inhomogeneously distributes at the cm-dm scale. However, the average of all the individual sample analyses shown in the plot, can be assumed to represent the average for the whole sample.

STEINKORSEN

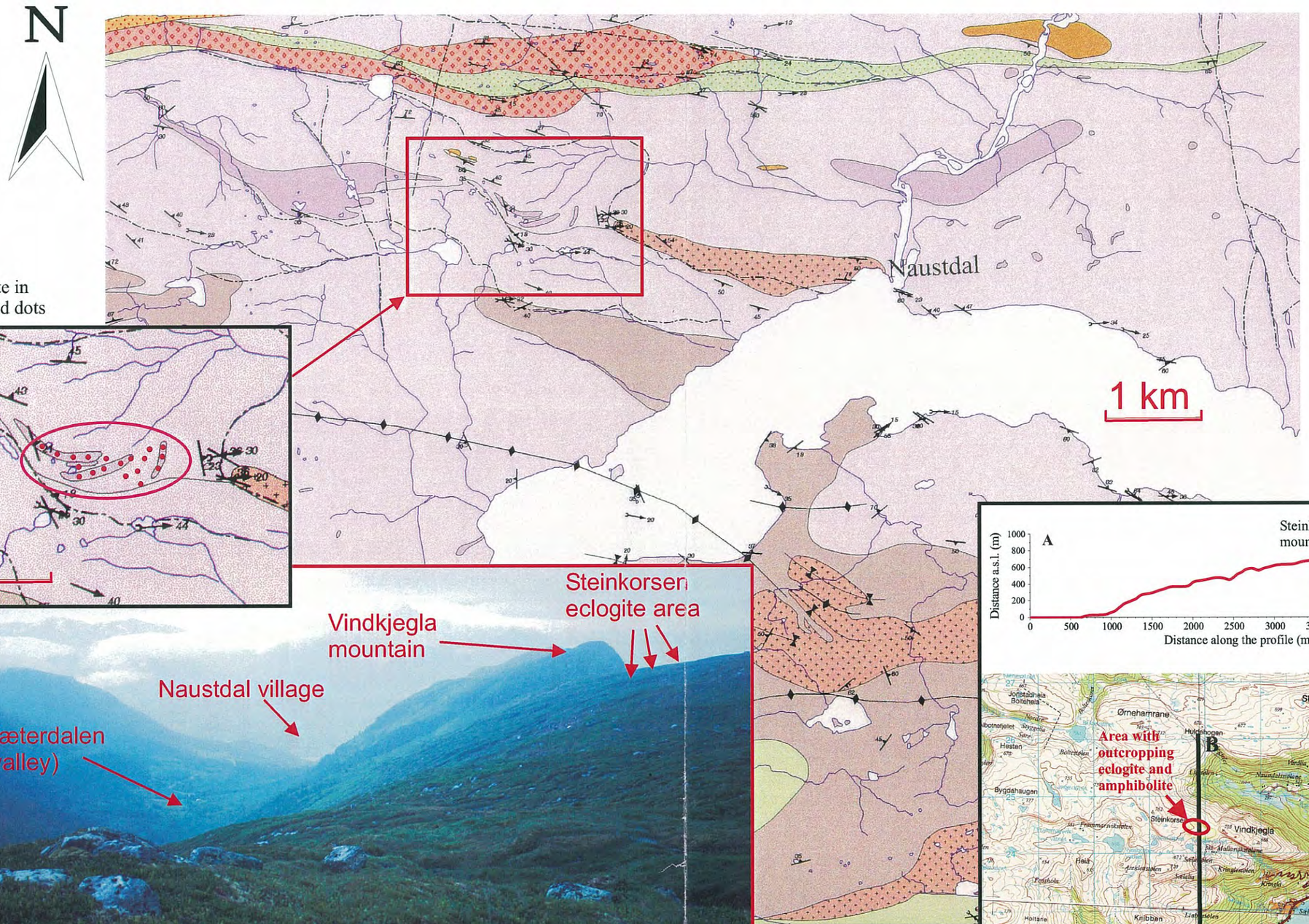

Fig. 31: Geographic and geological setting of the Steinkorsen eclogite.

Overview photograph of the Steinkorsen-Vindkjegla-Sæterdalen area viewed eastwards towards the Naustdal village

Vertical profile showing the assumed position of the Steinkorsen eclogite body (upper figure). The geographic position of the profile is shown by the lower figure.

STEINKORSEN

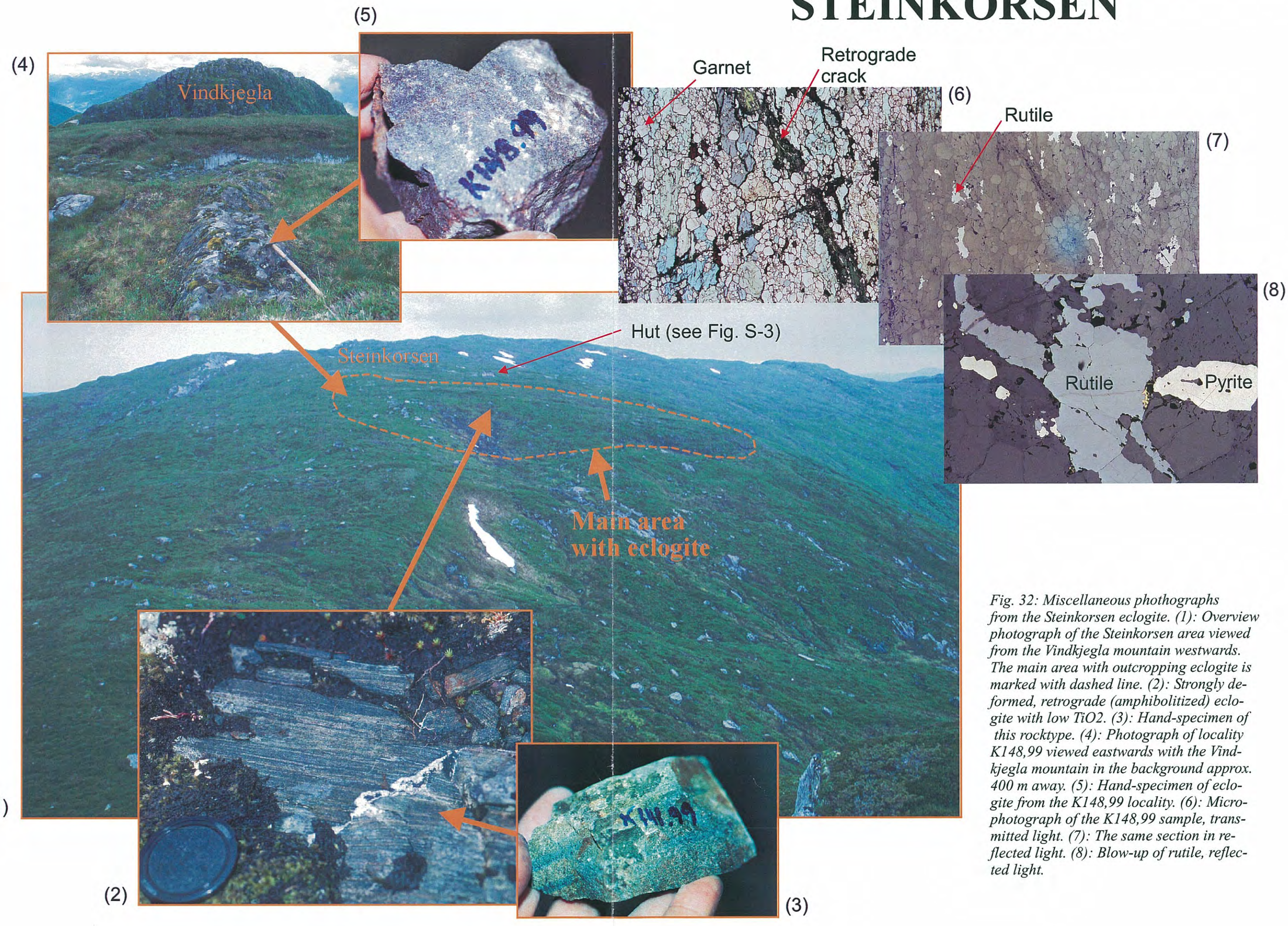

Fig. 32: Miscellaneous phothographs from the Steinkorsen eclogite. (1): Overview photograph of the Steinkorsen area viewed from the Vindkjegla mountain westwards. The main area with outcropping eclogite is marked with dashed line. (2): Strongly deformed, retrograde (amphibolitized) eclogite with low TiO2. (3): Hand-specimen of this rocktype. (4): Photograph of locality K148,99 viewed eastwards with the Vindkjegla mountain in the background approx. 400 m away. (5): Hand-specimen of eclogite from the K148,99 locality. (6): Microphotograph of the K148,99 sample, transmitted light. (7): The same section in reflected light. (8): Blow-up of rutile, reflected light.

STEINKORSEN

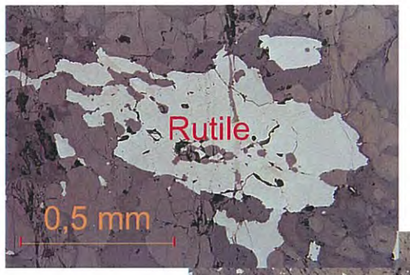

(7)

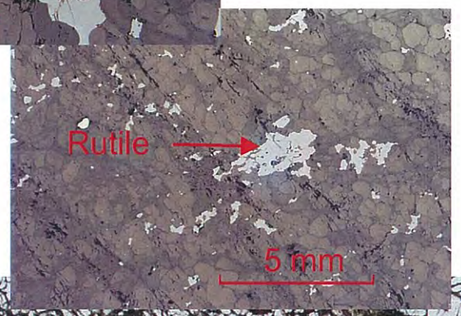

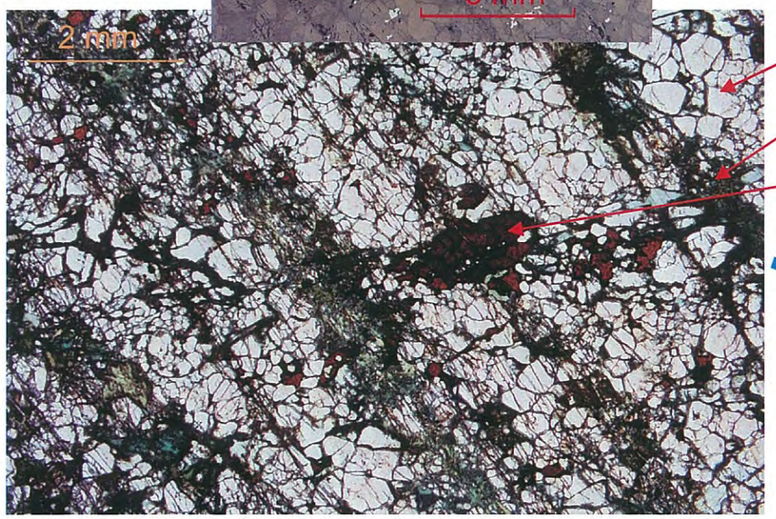

(5)

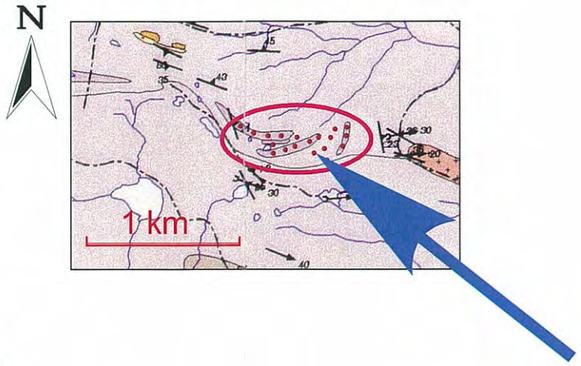

(4)

(3)

(2)

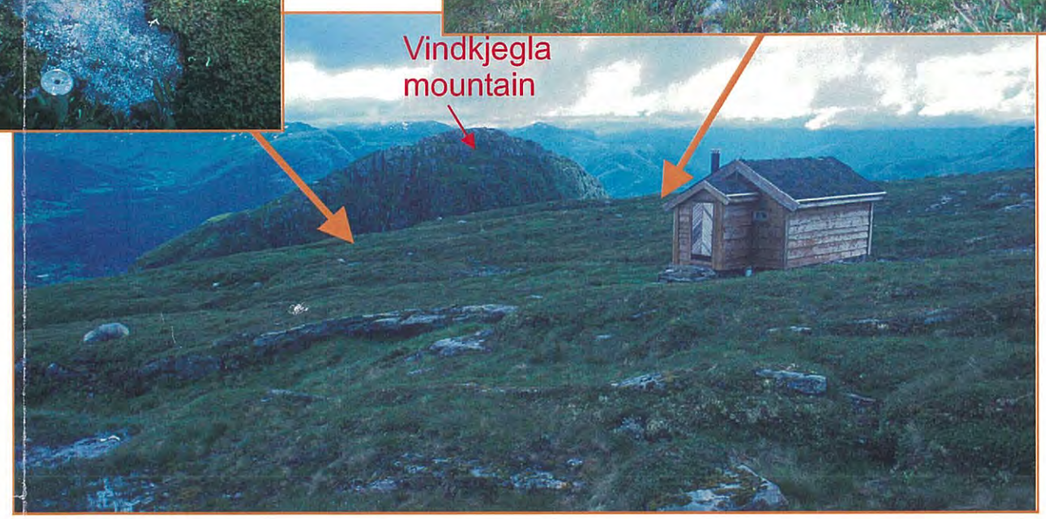

(1)

Fig. 33: Miscellaneous phothographs (continued) from the Steinkorsen eclogite. (Area 1): Overview photograph showing the area with outcropping eclogite in the foreground just behind the small hut. The distance from the hut to the Vindkjegla mountain in the background is approx. 0,5 km. The anomaly area with outcropping eclogite and amphibolite is from 50 m behind the hut and approx. 200 m towards Vindkjegla. (2): Eclogite locality K148,99. (3): Closeup photo of eclogite with large rutile crystals. (4): Eclogite with amphibolitization (retrogression) along cracks/veins. (5): Microphotograph of eclogite with distinct retrogression along cracks. Sample K147,99, transmitted light. (6): The same section viewed in reflected light. (7): Blow-up of large rutile grain from the previous image. Reflected light.

STEINKORSEN

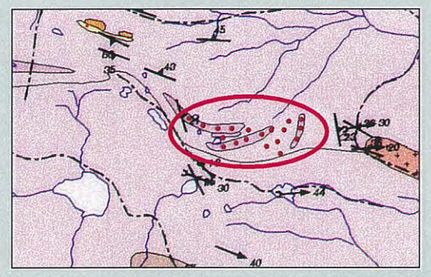

Geological map of the Steinkorsen area. Outcropping eclogite is marked with red dots.

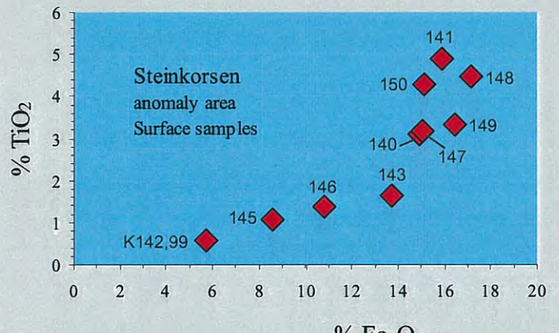

X-met analyses of chip-samples from Steinkorsen.
Each point represents an average of 5-10 subsamples.

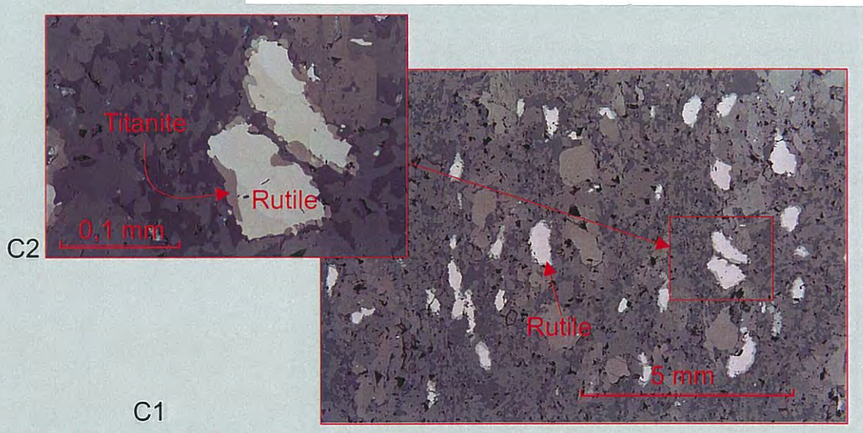

Microphotographs of eclogite sample K143,99, reflected light. This sample is significantly retrograded (amphibolitized) and rutile show beginning alteration to titanite at the rim.

Oxide grain-size distribution in eclogite thin-sections shown in two types of diagrams.

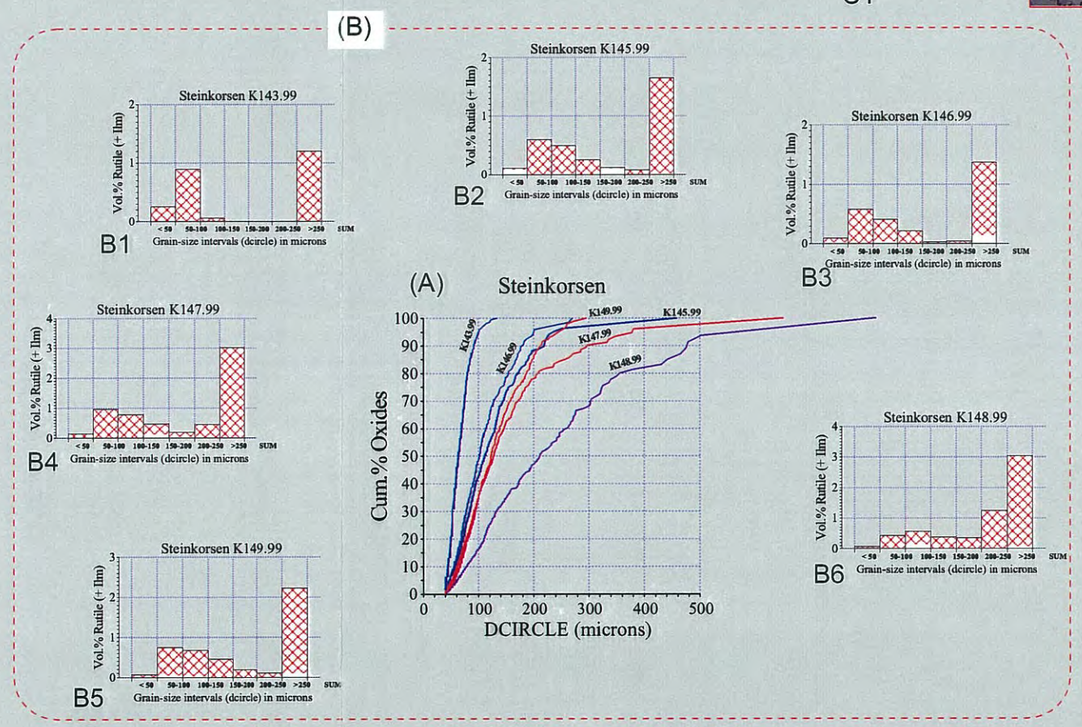

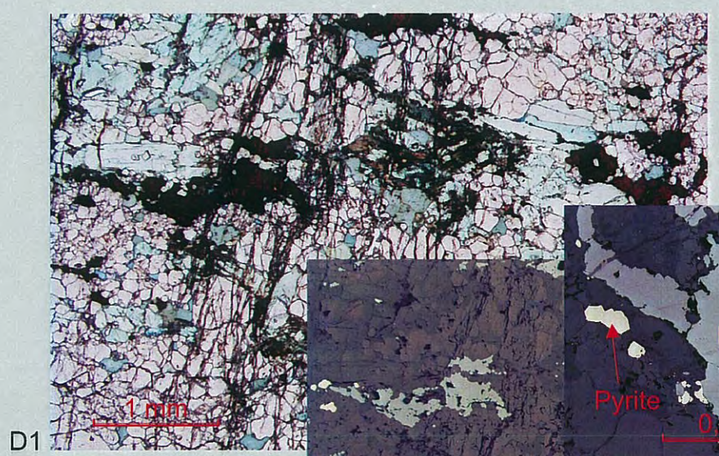

Transmitted light.
Sample K148,99

Reflected light

Reflected light

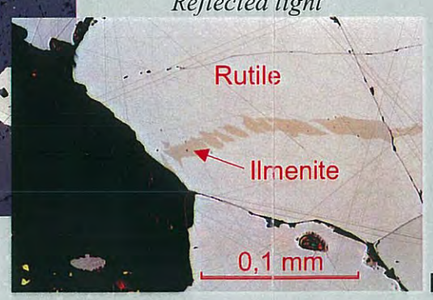

Microphotographs of eclogite sample K148,99

Fig. 34: Characterization of eclogite samples (thin-sections) from Steinkorsen. Fig. (A) shows the cumulative oxide grain-size distribution in 6 samples, while Figs. B1-B6 shows vol.% oxide (rutil ±ilm.) Vs. Grain-size intervals. The microphotographs C1 and C2 is of the heavy retrograded (amphibolitized) low-Ti eclogite K143,99 in which rutile is distinctly altered to titanite at the margin. The Microphotographs D1-D4 is of the eclogite sample K148,99 which is relatively rutile-rich and with large crystals.

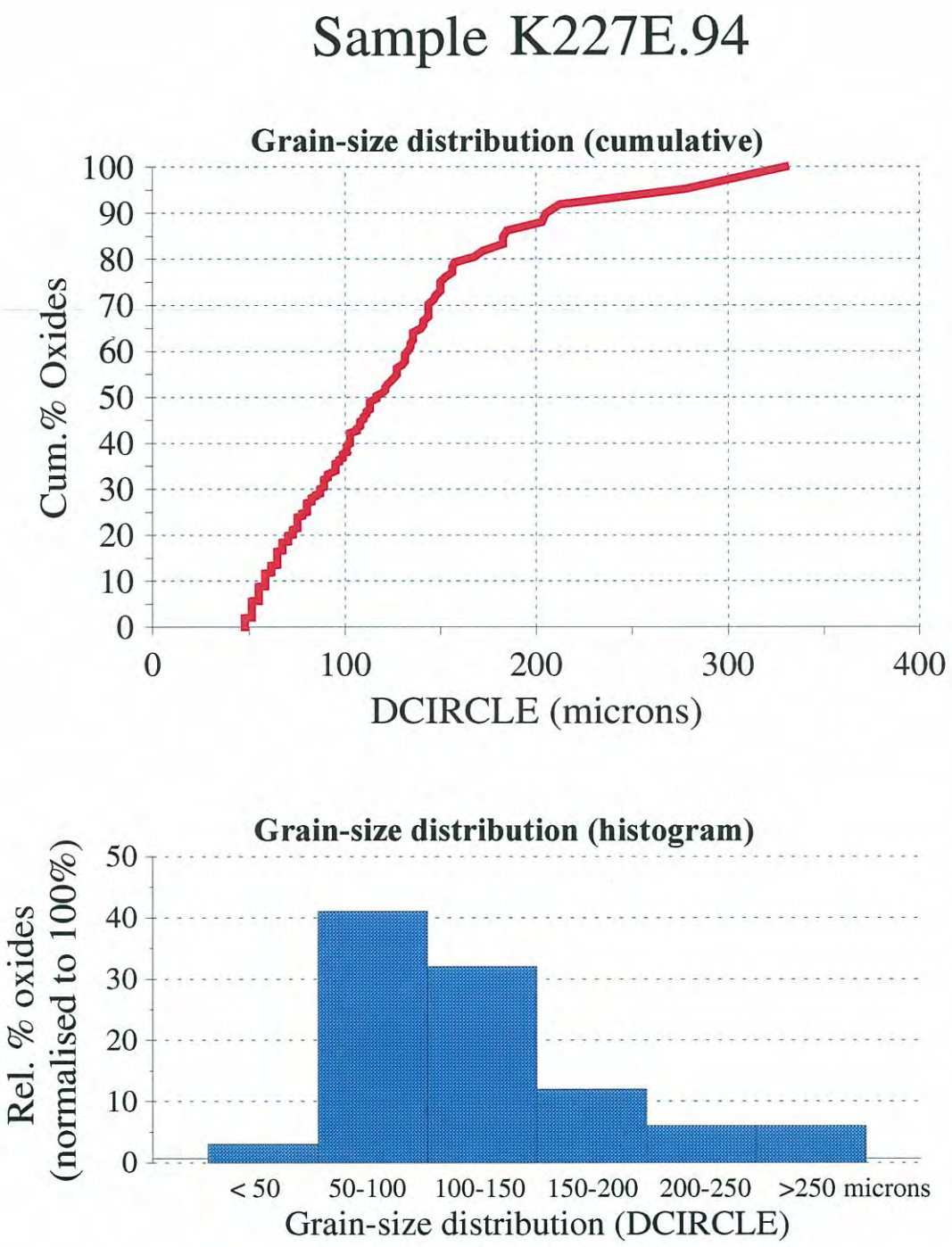

Fig. 35: Example showing the grain-size distribution of oxides (rutile + ilmenite) in a thin-sections from the Djupevatnet eclogite locality, Dalsfjord region.

(2)

Mineral data / Thin-section	Colour	4/120.9 (Engebøfj.)	304/69.9 (Engebøfj.)	K148.99 (Steink.)
Rutile	red	2.07 areal%	2.09 areal%	4.31 areal%
Ilmenite	blue	5.79 areal%	0.00 areal%	0.29 areal%
Apatite	green	0.19 areal%	0.21 areal%	0.01 areal%
Pyrite	yellow	0.69 areal%	0.16 areal%	0.26 areal%

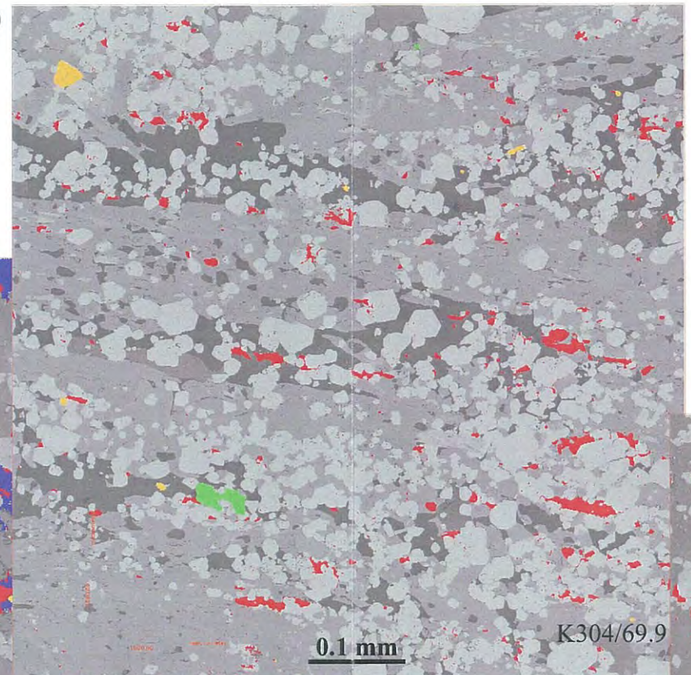

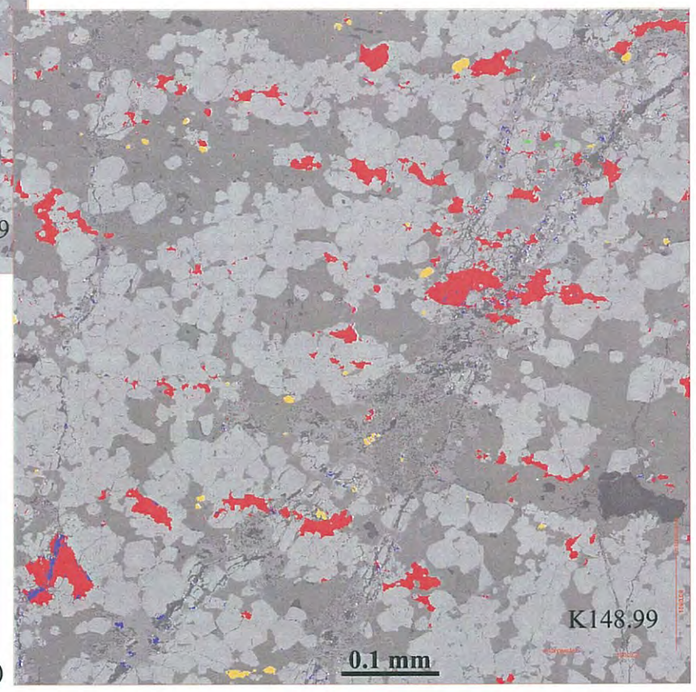

(3)

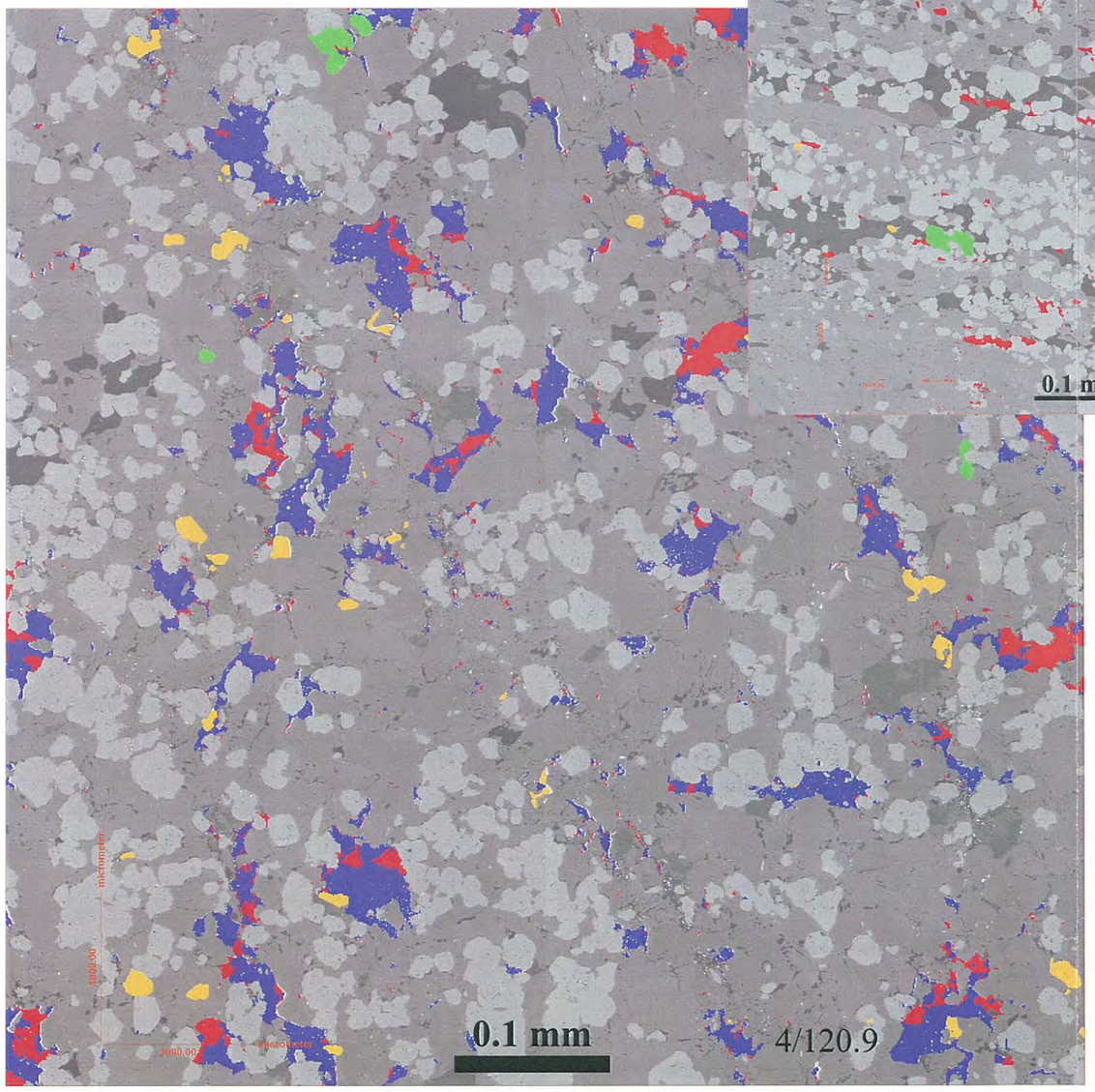

(1)

Fig. 36: Examples of the use of SEM-images in thin-section characterisation. Figure (1) is of a fairly altered eclogite sample from the Engebøfjellet eclogite in the Følrdefjord region (sample 4/120.9; Bh 4 at 120.9 m) with a high ilmenite to rutile ratio due to retrograde alteration under amphibolite facies conditions. Figure (2) is another sample from Engebøfjellet (sample 304/69.9 from Bh 304 at 69.9 m); this sample is practically unaffected by retrograde alteration and no ilmenite is present. Figure (3) is of sample K148.99 from the Orkheia eclogite, also in the Førdefjord region, showing ilmenite along fractures in which fluids have had access under amphibolite facies retrograde metamorphic conditions, leading to alteration of rutile to ilmenite.

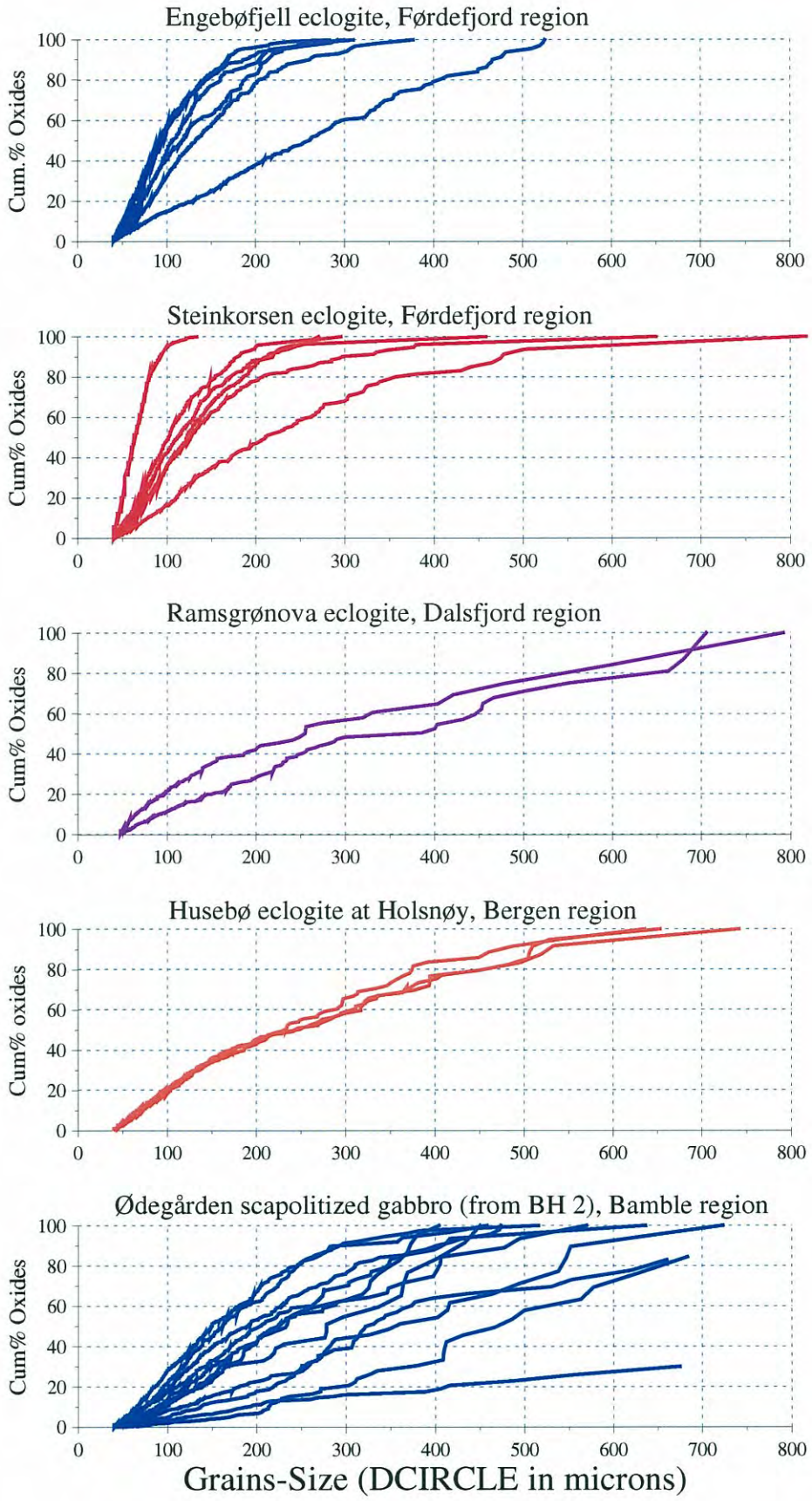

Fig. 37: Oxide grain-size distributions for some rutile deposits.

(5)

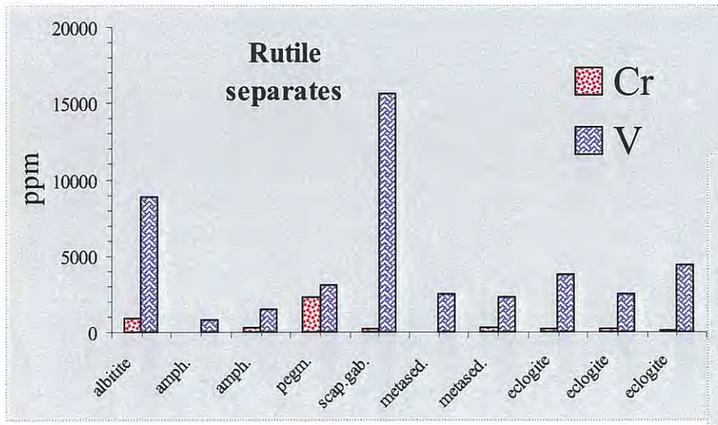

(4)

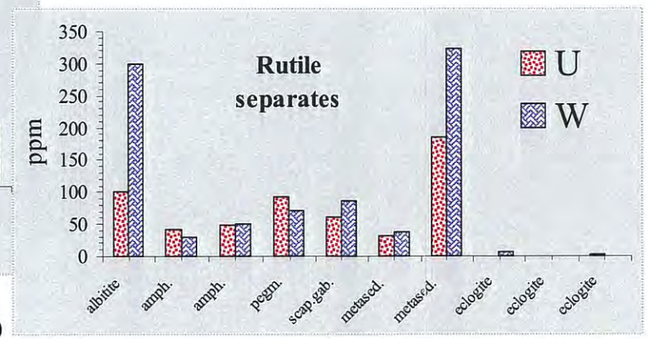

(1) XRF- and INA-analyses of rutile separates

Mineral consetrates made by a combinatioin of magnetic separation and heavy liquids at NGU (1991). Analysed by NGU (XRF) and Bondar Clegg, Canada (INAA) in 1992.

Locality		Vass botn	Vass botn	Saurdal	Saurdal	Husebø	Øde gård	Øde gård	Øde gård	Øde gård	Lindv. kollen	Hauk åsen	Gruve tjønn	Fone	Øde gård	Gjerstad vatnet
Sample		VB1A.91	VB1B.91	Sørdal-A	Sørdal-B	B	1¢66/79	2¢98/114	2¢120+	KB12H.91	KB11.91	KB9.91	KB6F.91	KB5F.91	KB37.91	KB43.91
Anal. no.		2	3	12	13	17	5	6	7	8	15	9	14	16	10	11
Mineral		rutile	rutile	rutile	rutile	rutile	rutile	rutile	rutile	rutile	rutile	rutile	rutile	rutile	rutile	rutile
Host-rock		ecl.	ecl.	ecl.	ecl.	ecl.	ødegårdite		phlog-enst-ap veins		albitite	pegm.	amph.	amph.	metased.	metased.
Region		Ålesund	Ålesund	Dalsfj.	Dalsfj.	Holsnøy	Bamble	Bamble	Bamble	Bamble	Bamble	Bamble	Bamble	Bamble	Bamble	Bamble
SiO2	*XRF (%)*	5.84	0.50	0.20	1.93	0.09	2.37	15.91	0.99	1.71	0.25	0.25	0.20	0.50	0.81	1.11
Al2O3	*XRF (%)*	2.97	0.18	0.09	0.52	0.03	0.38	0.06	0.14	0.00	0.08	0.13	0.00	0.07	0.36	0.32
Fe2O3	*XRF (%)*	7.11	0.65	5.52	3.33	2.98	0.19	11.51	0.35	0.44	0.85	0.10	0.67	1.27	1.04	1.13
TiO2	*XRF (%)*	79.95	95.59	92.68	91.59	95.54	91.64	40.43	95.70	94.41	96.87	97.12	97.94	97.39	95.29	94.51
MgO	*XRF (%)*	1.05	0.00	0.00	0.32	0.00	0.57	0.00	0.22	0.56	0.00	0.00	0.03	0.00	0.26	0.18
CaO	*XRF (%)*	1.45	0.28	0.27	0.79	0.22	0.55	0.48	0.35	0.22	0.31	0.00	0.41	0.54	0.19	0.24
Na2O	*XRF (%)*	0.00	0.00	0.00	2.96	1.12	0.00	0.00	0.47	0.00	0.00	0.00	0.00	0.00	0.00	0.00
K2O	*XRF (%)*	0.02	0.00	0.00	0.04	0.01	0.02	0.03	0.02	0.00	0.00	0.00	0.00	0.00	0.01	0.01
MnO	*XRF (%)*	0.07	0.00	0.00	0.00	0.00	0.00	0.00	0.00	0.00	0.00	0.00	0.00	0.00	0.00	0.00
P2O5	*XRF (%)*	0.00	0.00	0.00	0.00	0.00	0.05	0.07	0.00	0.00	0.00	0.00	0.00	0.00	0.02	0.00
Sum		*98.46*	*97.20*	*98.76*	*101.48*	*99.99*	*95.77*	*68.49*	*98.24*	*97.34*	*98.36*	*97.60*	*99.25*	*99.77*	*97.98*	*97.50*
Th	*INAA (ppm)*	1.0	0.7	-0.2	0.3	-0.2	8.9	32.2	na	1.6	0.6	1.8	0.9	0.9	1.3	1.6
U	*INAA (ppm)*	1.9	2.0	0.9	-0.2	0.3	61.4	121.0	na	56.0	100.0	93.2	48.8	42.0	184.0	31.4
Hf	*INAA (ppm)*	13	32	9	7	12	155	3130	na	36	42	81	15	49	59	109
Zr	*XRF (ppm)*	389	1232	228	181	399	6143	153523	2692	338	930	2454	580	1854	1422	4227
Nb	*XRF (ppm)*	113	135	39	33	84	326	390	686	1311	149	815	936	1775	806	434
Ta	*INAA (ppm)*	6	8	2	2	6	22	24	na	160	18	47	133	359	59	27
Y	*XRF (ppm)*	0	0	0	0	0	69	869	17	0	6	0	0	0	0	26
W	*INAA (ppm)*	-3	3	7	5	-1	85	13	na	174	300	72	51	30	322	37
Mo	*INAA (ppm)*	6	11	11	8	6	15	13	na	10	14	7	16	17	49	25
Sr	*XRF (ppm)*	19	11	0	28	134	14	0	0	0	10	0	11	6	22	7
Rb	*XRF (ppm)*	9	10	9	20	7	8	13	0	7	10	0	16	9	8	14
Pb	*XRF (ppm)*	0	0	0	0	0	16	32	0	0	0	0	26	0	0	65
Co	*XRF (ppm)*	33	-5	270	75	310	-5	460	na	-5	31	-5	-5	6	-5	23
Cr	*XRF (ppm)*	92	115	161	138	184	207	92	345	368	920	2323	276	46	345	46
Sc	*INAA (ppm)*	54	59	64	62	70	129	44	na	108	133	120	68	67	98	77
V	*XRF (ppm)*	4409	4588	3765	3678	2512	15635	982	10845	14295	8866	3072	1518	843	2290	2477
As	*INAA (ppm)*	-1	-1	2	-1	-1	4.7	19.0	na	-0.5	1.2	-0.5	-0.5	2.7	2.0	1.8
Sb	*INAA (ppm)*	0	0	4	4	0	4.5	3.1	na	4.0	11.4	1.6	2.6	5.8	61.3	4.9
La	*INAA (ppm)*	3	-2	-2	-2	-2	10	9	na	2	5	2	-2	3	3	4
Ce	*INAA (ppm)*	-22	18	-11	-11	-5	35	100	na	-20	-11	-12	-14	-19	-22	-15
Sm	*INAA (ppm)*	1	1	0	0	0	5.1	2.3	na	0.6	-2.5	-2.2	0.4	1.8	-4.5	0.4
Yb	*INAA (ppm)*	-2	-2	-2	-2	-2	9	154	na	-2	-2	-2	-2	-2	2	3

(2) Rutile concentrates analysed by Titania A/S (1991)

Mineral consetrates made by a combinatioin of magnetic separation and heavy liquids at NGU (1991).

Locality	Sannidal	Fone	Gruve tjønn	Lindv. Kollen	Engebø fjellet A	Engebø fjellet B	Engebø fjellet C	Husebø A	Husebø B	Ødegård
Sample										
Mineral	rutile	rutile	rutile	rutile	rutile	rutile	rutile	rutile	rutile	rutile
Host-rock	metased.	amph.	pegm.	albitite	eclog.	eclog.	eclog.	eclog.	eclog.	ødegårdite
Region	Bamble	Bamble	Bamble	Bamble	Førdefj.	Førdefj.	Førdefj.	Holsnøy	Holsnøy	Bamble
TiO2 (tot.)	92.06	96.48	97.41	95.34	92.88	95.38	96.35	91.91	93.80	95.70
% P2O5	0.06	0.01	0.01	0.03	0.01	0.01	0.01	0.01	0.01	0.01
% S	0.11	0.02	0.02	0.23	0.20	0.26	0.30	0.21	0.79	0.00
% Cr2O3	0.04	0.00	0.02	0.21	0.01	0.02	0.03	0.02	0.02	0.01
% SiO2	1.37	0.80	0.45	0.53	0.87	0.59	0.23	1.53	0.29	0.68
% V2O5	0.23	0.09	0.18	0.83	0.24	0.26	0.25	0.24	0.24	0.29
% CaO	0.05	0.45	0.30	0.14	0.20	0.10	0.03	0.49	0.06	0.39
% MgO	0.52	0.10	0.03	0.05	0.11	0.02	0.00	0.25	0.00	0.16
% Al2O3	1.07	0.59	0.49	0.81	0.80	0.57	0.45	0.95	0.48	-0.20
% Fe2O3	3.13	0.83	0.83	1.07	4.66	2.25	1.67	4.30	3.05	0.52
% Sum	*98.64*	*99.37*	*99.74*	*99.24*	*99.98*	*99.45*	*99.32*	*99.90*	*98.74*	*97.56*
TiO2 (HCl)	1.18	1.23	1.29	1.12	3.98	2.67	1.62	3.29	1.27	0.92
% Rutile	90.88	95.25	96.12	94.22	88.90	92.71	94.73	88.62	92.53	94.78

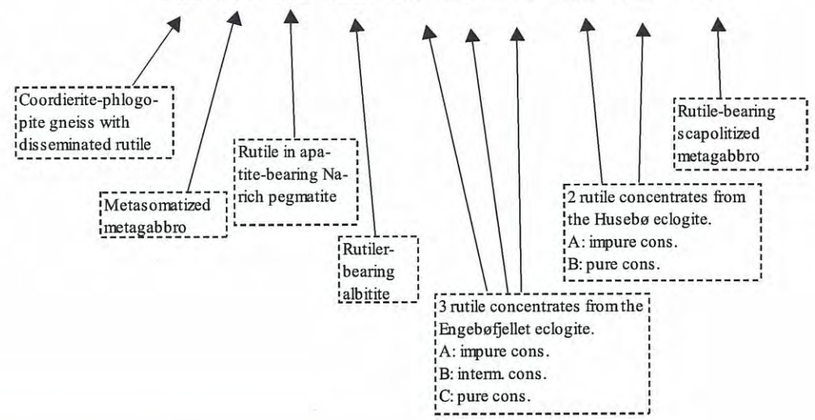

(3)

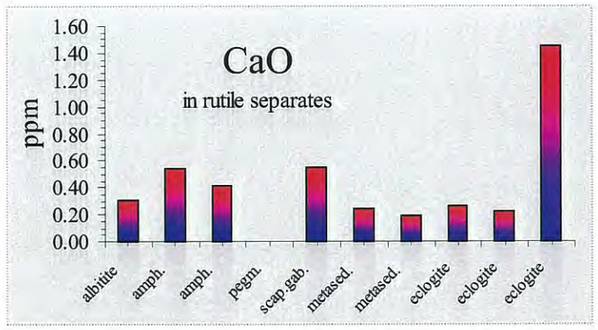

Fig. 38: Rutile analyses. Analyses of rutile separates from a variety of deposits are given in the two tables (1) and (2). The three graphs illustrates how the content of CaO (3), U and Th (4) and Cr and V (5) varies with deposit type.